In presenting the dissertation as a partial fulfillment of the requirements for an advanced degree from the Georgia Institute of Technology, I agree that the Library of the Institution shall make it available for inspection and circulation in accordance with its regulations governing materials of this type. I agree that permission to copy from, or to publish from, this dissertation may be granted by the professor under whose direction it was written, or, in his absence, by the dean of the Graduate Division when such copying or publication is solely for scholarly purposes and does not involve potential financial gain. It is understood that any copying from, or publication of, this dissertation which involves potential financial gain will not be allowed without written permission.

TRANSVERSE VIBRATION OF A CANTILEVERED CIRCULAR CYLINDRICAL SHELL

A THESIS

Presented to

The Faculty of the Graduate Division

by

Roy Mac Scruggs

In Partial Fulfillment

of the Requirements for the Degree

Master of Science in Engineering Mechanics

Georgia Institute of Technology

June, 1964

TRANSVERSE VIBRATION OF A CANTILEVERED CIRCULAR CYLINDRICAL SHELL

APPROVED:

Chairman

Date approved by Chairman: 5/1/64

ACKNOWLEDGMENTS

The author wishes to thank Dr. M. E. Raville for his guidance, interest and aid, which accelerated his work to completion.

The author is grateful to Drs. J. A. Stricklin and J. T. S. Wang for their reading of the manuscript and penetrating criticism of the problem involved.

Appreciation is especially extended to Mrs. Pat Davis for her speed and efficiency in typing the manuscript.

TABLE OF CONTENTS

LIST OF TABLES

LIST OF ILLUSTRATIONS

SUMMARY

The importance of thin shell structures has increased rapidly in recent years, both in the civil engineering and aerospace fields. An integral part of the design of most light shell structures is the vibration analysis, pursuant to various stability and load studies.

This study investigates the transverse vibration of a thin cantilevered circular cylindrical shell. A practical method of predicting the natural frequencies of vibration is developed and evaluated theoretically and verified experimentally.

The general approach is based on an energy principle. The strain energy of the shell is formulated based on classical first order theory, and the kinetic energy is similarly stated. A frequency determinant results after applying the variational process. Results are presented for eigenvalues as a function of geometry and mode number. Modal amplitudes are obtained and an explanation of eigenvalue distribution with mode number is made on the basis of energy distribution. The fact that for some shell lengths or axial mode numbers the modes having fewer circumferential nodes possess higher eigenvalues seems contrary to intuition, the reason for this behavior lies in the manner in which bending and "stretching" energy is distributed with mode number.

The results of a brief experimental investigation are presented and correlated with theoretical results. Sufficient agreement is found to verify the theory; further testing is recommended both for verification and to investigate boundary relaxation. In addition, analytical

work on boundary relaxation is needed to further increase the practical value of the method.

NOMENCLATURE

A_m	normalizing constant for m^{th} axial mode, radial and circumferential displacement
B_m	normalizing constant for m^{th} axial mode, axial displacement
E	Young's modulus of elasticity
L_1, L_2, L_3	constants occurring in frequency equation
M_m	modal constant for m^{th} axial mode
T	kinetic energy of shell
U, V, W	orthogonal displacements in shell surface, as functions of axial coordinate only
$\bar{U}$, $\bar{V}$, $\bar{W}$	generalized coordinates for shell displacements
a	mean radius of shell
b_{22}, b_{23}, b_{33}	constants occurring in L_1, L_2, L_3
h	shell thickness
ℓ	shell length
m	axial mode number
n	circumferential mode number
$s_{11}, s_{22}, s_{12}, s_{13}$, s_{21}, s_{31}	constants occurring in L_1, L_2, L_3
t	time
α_m	normalizing constant in m^{th} characteristic function of cantivelered beam
β	bending parameter, $h^2/12a^2$
γ	shearing strain, referred to shell middle surface

η	length ratio, a/ℓ
$\epsilon_x, \epsilon_y, \epsilon_{xy}$	general material strains, normal and shearing
ϵ_1, ϵ_2	normal strain in x,y directions referred to middle surface
$\sigma_x, \sigma_y, \sigma_{xy}$	general material stresses, normal and shearing
Ω	shell strain energy
θ	angular shell coordinate
K_1, K_2, K_{12}	incremental curvatures and twist of middle surface
Φ_m	characteristic function, m^{th} mode of uniform cantilevered beam
ρ	mass density
μ	equivalent wavelength parameter
ω	radian frequency
Δ	shell non-dimensional eigenvalue, $\rho \frac{a^2(1-\nu^2)}{E} \omega^2$
ν	Poisson's ratio
λ_m	modal parameter, m^{th} axial mode
γ_m	modal parameter, m^{th} axial mode
δ_S	energy factor for strain energy due to stretching and shearing
δ_B	energy factor for strain energy due to bending

CHAPTER I

INTRODUCTION

The free vibration of thin, circular cylindrical shells has been the subject of considerable study in the past. Some analyses have been carried to completion, notably those of Arnold and Warburton (4,5).*

The classical approach to the problem proceeding from the equilibrium equations, has consistently met with practical difficulties in generating eigenvalues for complex boundary conditions (6). Some questions also exist with reference to application of the available boundary conditions. The obvious advantage of using equilibrium equations is the generality available in obtaining solutions for any boundary conditions. The resulting numerical computations are necessarily tedious and lengthy. Several boundary conditions have been studied in the literature by energy methods, resulting in practically usable numerical methods for extracting eigenvalues. It is the purpose of this study to provide a solution for the cantilevered cylindrical shell, a problem not previously given detailed study, and to analyze the distribution of eigenvalues with geometry and mode number. An energy formulation is used, the kinetic and strain energies being obtained in terms of the shell displacements.

Considering a small element of the shell, as in Figure 1, the strain energy may be written to the first order as

---

*Numbers in parentheses after names refer to items in the Bibliography.

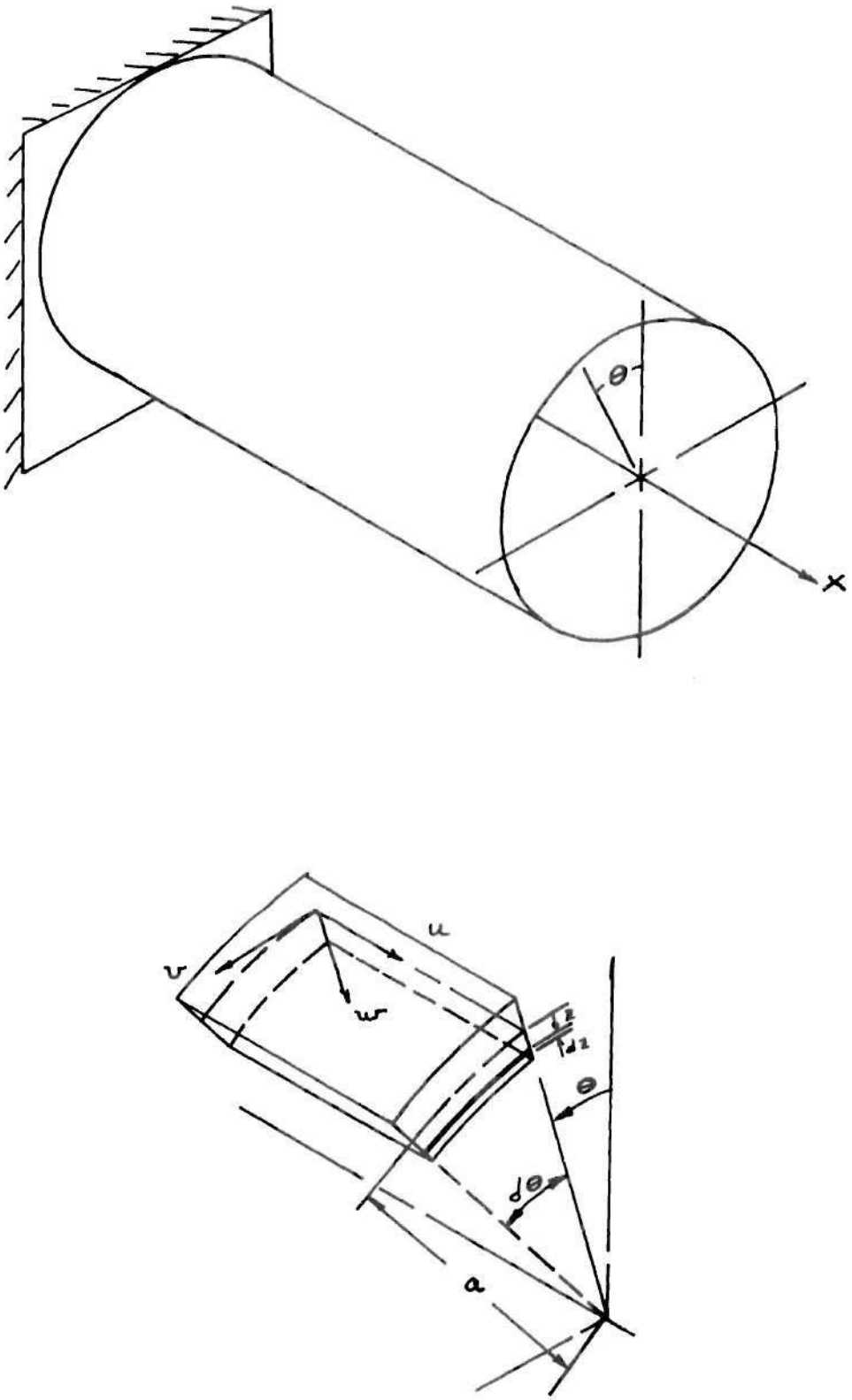

Figure 1. Shell Geometry And Coordinates

$$\Omega = \frac{1}{2}\int_0^{2\pi}\int_0^{\ell}\int_{-h/2}^{+h/2}\left(\sigma_x\epsilon_x + \sigma_y\epsilon_y + \sigma_{xy}\epsilon_{xy}\right)a\,dz\,d\theta\,dx \qquad (1)$$

where, consistent with the Love-Kirchoff assumption, the normal stress and shearing stresses σ_{xz}, σ_{yz}, are neglected. Also the trapezoidal shape of the faces perpendicular to the x axis have been neglected. Applying Hooke's Law, the energy in terms of strain only becomes

$$\Omega = \frac{E}{2(1-\nu^2)}\int_0^{2\pi}\int_0^{\ell}\int_{-h/2}^{+h/2}\left[\epsilon_x^2 + \epsilon_y^2 + 2\nu\epsilon_x\epsilon_y + \frac{(1-\nu)}{2}\epsilon_{xy}^2\right]a\,d\theta\,dx\,dz \qquad (2)$$

First order expansion of the strains in terms of average direct strains and changes of curvature in the coordinate directions gives the following equations, after Timoshenko (1):

$$\left.\begin{aligned} \epsilon_x &= \epsilon_1 - z\,K_1 \qquad & \epsilon_y &= \epsilon_2 - z\,K_2 \\ & & \epsilon_{xy} &= \gamma - 2z\,K_{12} \end{aligned}\right\} \qquad (3)$$

Referring to displacements u, v, w, of the middle surface, the strains and curvatures in Equations (3) are, to first order,

$$\epsilon_1 = \frac{\partial u}{\partial x} \quad , \quad \epsilon_2 = \frac{1}{a}\frac{\partial v}{\partial \theta} - \frac{w}{a} \quad , \quad \epsilon_{12} = \frac{\partial v}{\partial x} + \frac{1}{a}\frac{\partial u}{\partial \theta} \qquad (4)$$

$$K_1 = \frac{\partial^2 w}{\partial x^2} \quad , \quad K_2 = \frac{1}{a^2}\frac{\partial^2 w}{\partial \theta^2} + \frac{1}{a^2}\frac{\partial v}{\partial \theta} \quad , \quad K_{12} = \frac{1}{a}\frac{\partial^2 w}{\partial x\,\partial \theta} + \frac{1}{a}\frac{\partial v}{\partial x}$$

Substituting Equations (4) into Equations (3) and the resulting expressions into Equation (2) provides an expression directly integrable in z. The strain energy then becomes,

$$\Omega = \frac{E a h}{2(1-\nu^2)} \int_0^{2\pi} \int_0^{\ell} \left\{ \frac{1}{a^2}\left(a \frac{\partial u}{\partial x} + \frac{\partial v}{\partial \theta} - w \right)^2 - \frac{2(1-\nu)}{a} \frac{\partial u}{\partial x}\left(\frac{\partial v}{\partial \theta} - w \right) \right. \quad (5)$$

$$+ \frac{(1-\nu)}{2a^2}\left(a \frac{\partial v}{\partial x} + \frac{\partial u}{\partial \theta} \right)^2 + \beta \left[\frac{1}{a^2}\left(a^2 \frac{\partial^2 w}{\partial x^2} + \frac{\partial^2 w}{\partial \theta^2} + \frac{\partial v}{\partial \theta} \right)^2 \right.$$

$$\left. \left. - 2(1-\nu) \frac{\partial^2 w}{\partial x^2}\left(\frac{\partial^2 w}{\partial \theta^2} + \frac{\partial v}{\partial \theta} \right) + 2(1-\nu)\left(\frac{\partial^2 w}{\partial x \partial \theta} + \frac{\partial v}{\partial x} \right)^2 \right] \right\} d\theta\, dx$$

where $\beta = \frac{h^2}{12 a^2}$. Equation (5) agrees with that given by Timoshenko (1). It is noted that the result in Equation (5) is not exact to first order, since a first variation of the integral does not provide the accepted equilibrium equations for a circular cylindrical shell, as given for example by Flugge (8). Bleich and Dimaggio (9) have obtained an energy integral which does provide the exact equilibrium equations on application of the extremum principle. In deriving Equation (5), the change in length of circumferential fibers through the thickness of the shell was neglected. Bleich and Dimaggio included this effect and the resulting energy integral appears different in some of the bending terms when compared to Equation (5). For most practical purposes Equation (5) is found to give good results. In particular, Arnold and Warburton (4), made comparisons for thin shell vibrations and found a negligible effect due to consideration of the change of circumferential fiber length

through the shell thickness. For the range of circumferential mode numbers considered in the present study, Equation (5) is considered to be adequate to represent the strain energy.

Considering the mass of a shell element to be compressed into the middle surface neglects only small inertial couples about the middle surface axes, and these couples may be neglected for a thin shell with a practical limit on the number of circumferential nodes. Thus, the first order expression for kinetic energy is

$$T = \frac{1}{2}\rho a h \int_0^{2\pi} \int_0^{\ell} \left\{ \left(\frac{\partial u}{\partial t}\right)^2 + \left(\frac{\partial v}{\partial t}\right)^2 + \left(\frac{\partial w}{\partial t}\right)^2 \right\} d\theta\, dx \qquad (6)$$

Equations (5) and (6), along with the boundary conditions, permit analysis of the small vibrations of any thin circular cylindrical shell, upon application of a variational principle, or equivalently, direct use of Lagrange's equations.

CHAPTER II

VIBRATION ANALYSIS OF THE CANTILEVERED SHELL

The variational principle to be applied is Hamilton's Principle, $\delta($ - = 0. Configuration functions are chosen which satisfy the kinematic boundary conditions and are considered to give reasonable approximations to the state of strain in the shell. General experience with this procedure indicates that the eigenvalues are not greatly sensitive to the detailed shape of such assumed functions, so long as the boundary values are satisfied. Having established generalized coordinates, Lagrange's equations may be applied directly.

The appropriate boundary conditions for the cantilever are:

$$\left.\begin{aligned} u = v = w = 0 \\ \frac{\partial w}{\partial x} = 0 \end{aligned}\right\} \text{AT } x = 0 \tag{7}$$

The displacements are assumed in the following separated form,

$$\left.\begin{aligned} u &= U(x,t)\cos n\theta \\ v &= V(x,t)\sin n\theta \\ w &= W(x,t)\cos n\theta \end{aligned}\right\} \tag{8}$$

The strain energy in terms if U, V, and W then becomes,

$$\Omega = \frac{Eh\pi a}{2(1-\nu^2)} \int_0^{\ell} \left\{ \frac{1}{a^2}(aU' + nV - W)^2 - \frac{2(1-\nu)}{a} U'(nV - W) \right. \tag{9}$$

$$+ \frac{(1-\nu)}{2a^2}(aV' - nU)^2 + \beta \left[\frac{1}{a^2}(a^2W'' - n^2W + nV)^2 \right.$$

$$\left. \left. - 2(1-\nu)W''(nV - n^2W) + 2(1-\nu)(V' - nW')^2 \right] \right\} dx$$

The characteristic functions for a uniform cantilevered beam will be used to approximate the x component of the shell displacements; these functions are of the form

$$\Phi_m = \cosh \frac{\mu x}{a} - \cos \frac{\mu x}{a} - \alpha_m \left(\sinh \frac{\mu x}{a} - \sin \frac{\mu x}{a} \right) \tag{10}$$

where μ and α_m are known values for each m, (7).

$$\left.\begin{aligned} U &= \overline{U} B_m \frac{a}{\mu} \frac{d\Phi_m}{dx} \\ V &= \overline{V} A_m \Phi_m \\ W &= \overline{W} A_m \Phi_m \end{aligned}\right\} \tag{11}$$

where $\overline{U}$, $\overline{V}$, $\overline{W}$, are generalized coordinates referred to $x = \ell$. A_m and B_m are normalizing constants used for computational convenience in applying the data of Young and Felgar (7). It is noted that the functions representing V(x) and W(x) are orthogonal over the range $(0,\ell)$, but the derivative of these functions, while satisfying the boundary conditions on U(x) and $\frac{dU}{dx}$, do not form an orthogonal set. However, consistent with

the functions representing V and W, the functions $d\Phi/dx$ are a reasonable approximation to U, and the cross terms resulting from the lack of orthogonality will be neglected in computing the energy expressions.

The strain energy becomes,

$$\Omega = \frac{Eh\pi a}{2(1-\nu^2)} \int_0^\ell \left\{ \frac{1}{a^2} \left(\frac{a^2}{\mu} B_m \Phi_m'' \bar{U} + n A_m \Phi_m \bar{V} - A_m \Phi_m \bar{W} \right)^2 \right. \tag{12}$$

$$- \frac{2(1-\nu)}{\mu} A_m B_m \Phi_m \Phi_m'' (n\bar{V} - \bar{W}) \bar{U} + \frac{(1-\nu)}{2} \Phi_m'^2 \left(A_m \bar{V} - n \frac{B_m}{\mu} \bar{U} \right)^2$$

$$+ \beta \left[\frac{1}{a^2} A_m^2 \left(a^2 \Phi_m'' \bar{W} - n^2 \Phi_m \bar{W} + n \Phi_m \bar{V} \right)^2 \right.$$

$$\left. \left. - 2(1-\nu) n A_m^2 \Phi_m \Phi_m'' (\bar{V} - n\bar{W}) \bar{W} + 2(1-\nu) A_m^2 \Phi_m'^2 (\bar{V} - n\bar{W})^2 \right] \right\} dx$$

The kinetic energy is,

$$T = \frac{1}{2} \rho h \pi a \int_0^\ell \left\{ B_m^2 \frac{a^2}{\mu^2} \Phi_m'^2 \dot{\bar{U}}^2 + A_m^2 \Phi_m^2 \dot{\bar{V}}^2 + A_m^2 \Phi_m^2 \dot{\bar{W}}^2 \right\} dx \tag{13}$$

Lagrange's equations are applied as follows

$$\left. \begin{aligned} \frac{d}{dt} \frac{\partial T}{\partial \dot{\bar{U}}} + \frac{\partial \Omega}{\partial \bar{U}} &= 0 \\ \frac{d}{dt} \frac{\partial T}{\partial \dot{\bar{V}}} + \frac{\partial \Omega}{\partial \bar{V}} &= 0 \\ \frac{d}{dt} \frac{\partial T}{\partial \dot{\bar{W}}} + \frac{\partial \Omega}{\partial \bar{W}} &= 0 \end{aligned} \right\} \tag{14}$$

Setting

$$\left.\begin{aligned} \ddot{\bar{U}} &= -\omega^2 \bar{U} \\ \ddot{\bar{V}} &= -\omega^2 \bar{V} \\ \ddot{\bar{W}} &= -\omega^2 \bar{W} \end{aligned}\right\} \tag{15}$$

in Equations (14) results in a third order characteristic determinant. Defining the frequency parameter,

$$\Delta = \frac{\rho a^2 (1-\nu^2)\omega^2}{E} \tag{16}$$

the following cubic in Δ is found,

$$\Delta^3 - L_1 \Delta^2 + L_2 \Delta - L_3 = 0 \tag{17}$$

where

$$L_1 = 1 + s_{11} + s_{22} + \beta (b_{22} + b_{33}) \tag{18}$$

$$L_2 = s_{11} + s_{22} + s_{11} s_{22} - s_{12} s_{21} - n^2 - s_{13} s_{31} + \beta (b_{22} + s_{11} b_{22} + s_{11} b_{33} + s_{22} b_{33} + 2n b_{23}) \tag{19}$$

$$\begin{aligned} L_3 = {} & s_{11} s_{22} - n s_{12} s_{31} - n s_{21} s_{13} - s_{12} s_{21} - n^2 s_{11} \\ & - s_{13} s_{31} s_{22} + \beta (s_{11} b_{22} + s_{11} s_{22} b_{33} \\ & + s_{12} s_{31} b_{23} + s_{21} s_{13} b_{23} + 2n s_{11} b_{23} \\ & - s_{21} s_{12} b_{33} - s_{13} s_{31} b_{22}) \end{aligned} \tag{20}$$

and

$$S_{11} = \frac{\eta^2 \lambda_m^3}{(\rho_m - M_m)} + n^2 \frac{(1-\nu)}{2} \tag{21a}$$

$$S_{12} = \frac{\nu n M_m}{(\rho_m - M_m)} - n \frac{(1-\nu)}{2} \tag{21b}$$

$$S_{13} = -\frac{\nu M_m}{(\rho_m - M_m)} \tag{21c}$$

$$S_{21} = \eta^2 n \lambda_m \left[\frac{(1+\nu)}{2} M_m - \frac{(1-\nu)}{2} \rho_m \right] \tag{21d}$$

$$S_{31} = -\nu \eta^2 \lambda_m M_m \tag{21e}$$

$$S_{22} = n^2 + \eta^2 \lambda_m \frac{(1-\nu)}{2} (\rho_m - M_m) \tag{21f}$$

$$b_{22} = n^2 + 2\eta^2 \lambda_m (1-\nu)(\rho_m - M_m) \tag{21g}$$

$$b_{23} = -n^3 + (2-\nu)\eta^2 n \lambda_m M_m - 2(1-\nu)\eta^2 n \lambda_m \rho_m \tag{21h}$$

$$b_{33} = n^4 + \eta^4 \lambda_m^4 + 2(1-\nu)\eta^2 n^2 \lambda_m \rho_m - 2\eta^2 n^2 \lambda_m M_m \tag{21i}$$

The parameter λ_m the argument of the characteristic functions evaluated at $x = \ell$, is obtained from the tabulated data for a cantilevered beam as given in Reference 7; ρ_m is also obtained from the referenced tables as twice the absolute value of the slope function,

and M_m is defined as follows,

$$M_m = \frac{1}{4}\left\{(1+\alpha_m^2)\sinh 2\lambda_m - 2\alpha_m \cosh 2\lambda_m \right. \tag{22}$$
$$-(1-\alpha_m^2)\sin 2\lambda_m - 2\alpha_m \cos 2\lambda_m$$
$$\left. - 4\alpha_m^2 \lambda_m + 4\alpha_m \right\}$$

The parameters λ_m, f_m, M_n, A_m, and B_m are presented in Table 1 for the first five axial modes.

The frequency parameter Δ may now be computed from Equation (17), given only the two geometric ratios η and β, where $\eta = \frac{a}{\ell}$, and Poisson's ratio, ν.

The modal amplitudes are determined from the frequency determinant by substituting known values of Δ and solving any two of the equations for the ratios $\bar{U}/\bar{W}$ and $\bar{V}/\bar{W}$. The resulting relations are

$$\frac{\bar{U}}{\bar{W}} = \frac{\eta \lambda_m A_m}{D B_m}\left\{ s_{13}\Delta + \beta(s_{12}b_{23} - s_{13}b_{22}) \right. \tag{23}$$
$$\left. - s_{13}s_{22} - n s_{12} \right\}$$

$$\frac{\bar{V}}{\bar{W}} = \frac{1}{D}\left\{(\beta b_{23} - n)\Delta - s_{11}(\beta b_{23} - n)\right\} \tag{24}$$

where

$$D = \Delta^2 - (s_{11} + s_{22} + \beta b_{22})\Delta \tag{25}$$
$$+ s_{11}s_{22} - s_{12}s_{21} + \beta s_{11} b_{22}$$

Table 1. Parameters Representing Five Axial Modes

m	λ_m	f_m	M_m	A_m	B_m
1	1.87510	2.93638	.45767	.500	.68111
2	4.69410	4.07386	-3.33265	.500	.49093
3	7.85480	3.99690	-6.34372	.500	.50038
4	10.99550	4.00014	-9.49611	.500	.49998
5	14.13720	4.00000	-12.63720	.500	.50000

NOTE: For $m > 5$,

$$\lambda_m \approx (2m-1)\frac{\pi}{2}$$

$$\alpha_m \approx 1.00000$$

$$A_m = B_m \approx .50000$$

$$f_m \approx 4.00000$$

For any m, n combination, Equation (17) provides three real positive values for Δ. Thus for each modal pattern three eigenvalues are defined. However, the relative amplitudes of the three displacement components is different for each value. For any practical case, only one of the eigenvalues is of interest, the other two being extremely large. Typical numerical values for these frequencies will be presented in a later section. For the range of parameters considered in this study, the terms Δ^3 and $L_1\Delta^2$ in Equation (17) are small compared to the other terms. The following relation, which is obtained as a second approximation from Equation (17), gives good approximations to the lower value of Δ,

$$\Delta \approx \frac{L_3}{L_2} + \frac{L_1}{L_2}\left(\frac{L_3}{L_2}\right)^2 \qquad (26)$$

Extensive calculations have been made for cylinders with various thickness to radius ratios, h/a, and radius to length ratios, η. Computations for h/a = .002 and h/a = .020 are presented here for analysis and comparison. Figure 2 presents plotted data for the frequency factor $\sqrt{\Delta}$ versus wavelength factor μ, with the circumferential mode number as a parameter, for h/a = .020. The quantity μ does not directly indicate the axial wavelength for an axial wave pattern, since the deformations for a cantilevered shell are not simply sinusoidal. It is equivalent to the factor $\frac{m\pi a}{\ell}$ occurring in the case of a simply supported shell, (4), and is useful for presenting data. For a particular axial mode, the value of λ_m is known from Table 1 and μ is obtained as the product of λ_m and η. From the standpoint of design usage, it may be desirable to

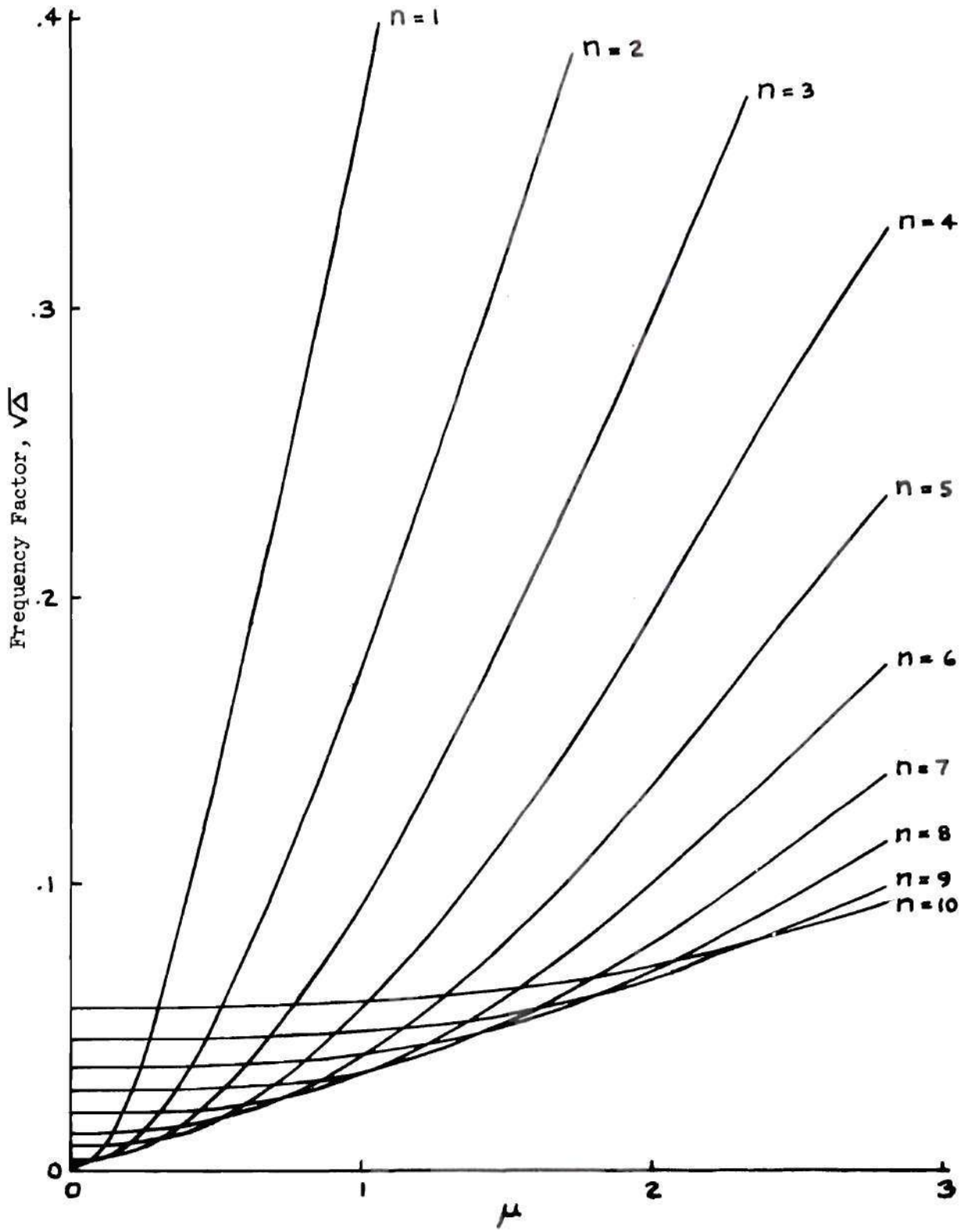

Figure 2. Frequency Factor For h/a = .002.

obtain frequencies as a function of η only, for given axial and circumferential mode numbers. This is provided as additional information in Appendix A for the thickness ratios previously mentioned. Table 2 (a, b) presents sample calculations of modal amplitudes $\bar{U}/\bar{W}$ for h/a = .002 at η = .100 and η = .500 respectively. Similar calculations are presented in Table 3, (a, b) for h/a = .020. Appendix A contains additional computations for η = .167 and η = .250. It is noted that for all axial mode numbers the ratio $\bar{V}/\bar{W}$ approaches 1/n as n becomes large. This is expected since the modes approach the inextensional condition, for which theory predicts $\bar{V}/\bar{W}$ = 1/n, $\bar{U}/\bar{W}$ = 0. It is further noted that the axial displacement $\bar{U}$, which is the primary stretching displacement, is significant for m = 1 at η = .500 for the low values of n, being of the order of 10-15 per cent of the primary radial term w. This fact will be related to certain experimental difficulties discussed in a later section. The frequency "crossover" trend of modes with lower n, known to exist for shells with other boundary conditions (4), is apparent for the cantilevered condition from a study of Figures 2 and 3. Thus for h/a = .002 at μ = 1.0, the frequency for the n = 10 mode is about 30 per cent of that for n = 2. This phenomenon is more evident for the thinner shell, as comparison of Figures 2 and 3 shows. The fact that more complex modal patterns sometimes possess lower eigenvalues may be explained by considering the distribution of strain energy in the various modes. Equation (11) reflects two basic mechanisms for storing elastic strain energy. The first part is due to "stretching" that results from membrane strain in the middle surface. The part multiplying β is composed of bending and twisting terms which are

Table 2. Relative Modal Amplitudes, h/a = .002

(a) $\eta = .100$

	m = 1		m = 2		m = 3		m = 4		m = 5	
n	$\bar{U}/\bar{W}$	$\bar{V}/\bar{W}$	$\bar{U}/\bar{W}$	$\bar{V}/\bar{W}$	$\bar{U}/\bar{W}$	$\bar{V}/\bar{W}$	$\bar{U}/\bar{W}$	$\bar{V}/\bar{W}$	$\bar{U}/\bar{W}$	$\bar{V}/\bar{W}$
1	.1278	.9950	.3628	1.0713	.3665	1.1142	.2807	1.0647	.1737	.9304
2	.0338	.4994	.1101	.5119	.1515	.5304	.1652	.5435	.1567	.5412
3	.0152	.3332	.0512	.3372	.0773	.3447	.0956	.3535	.1046	.3602
4	.0085	.2499	.0293	.2517	.0458	.2552	.0597	.2601	.0696	.2651
5	.0055	.2000	.0819	.2009	.0300	.2028	.0402	.2056	.0484	.2089
6	.0038	.1667	.0132	.1672	.0211	.1683	.0287	.1701	.0352	.1722
7	.0028	.1429	.0097	.1432	.0157	.1439	.0214	.1451	.0266	.1465
8	.0022	.1250	.0074	.1252	.0121	.1257	.0166	.1265	.0208	.1275
9	.0017	.1111	.0059	.1113	.0096	.1116	.0132	.1122	.0166	.1129
10	.0014	.1000	.0048	.1001	.0078	.1004	.0108	.1008	.0136	.1013

(b) $\eta = .500$

	m = 1		m = 2		m = 3		m = 4		m = 5	
n	$\bar{U}/\bar{W}$	$\bar{V}/\bar{W}$	$\bar{U}/\bar{W}$	$\bar{V}/\bar{W}$	$\bar{U}/\bar{W}$	$\bar{V}/\bar{W}$	$\bar{U}/\bar{W}$	$\bar{V}/\bar{W}$	$\bar{U}/\bar{W}$	$\bar{V}/\bar{W}$
1	.2367	.8465	.0046	.3716	-.0416	.1481	-.0399	.0793	-.0345	.0495
2	.1446	.4770	.1109	.4078	.0074	.2316	-.0179	.1390	-.0232	.0911
3	.0626	.3275	.1122	.3312	.0429	.2479	.0061	.1710	-.0087	.1202
4	.0383	.2477	.0897	.2606	.0572	.2294	.0244	.1795	.0053	.1360
5	.0255	.1989	.0686	.2099	.0581	.2014	.0350	.1733	.0163	.1410
6	.0181	.1661	.0526	.1742	.0532	.1744	.0393	.1604	.0238	.1385
7	.0135	.1425	.0411	.1484	.0468	.1515	.0397	.1456	.0280	.1318
8	.0104	.1248	.0328	.1291	.0404	.1329	.0379	.1313	.0299	.1232
9	.0083	.1110	.0266	.1142	.0347	.1179	.0350	.1184	.0300	.1140
10	.0068	.1000	.0220	.1023	.0299	.1056	.0320	.1072	.0292	.1052

Table 3. Relative Modal Amplitudes, h/a = .020

(a) η = .100

	m = 1		m = 2		m = 3		m = 4		m = 5	
n	$\bar{U}/\bar{W}$	$\bar{V}/\bar{W}$	$\bar{U}/\bar{W}$	$\bar{V}/\bar{W}$	$\bar{U}/\bar{W}$	$\bar{V}/\bar{W}$	$\bar{U}/\bar{W}$	$\bar{V}/\bar{W}$	$\bar{U}/\bar{W}$	$\bar{V}/\bar{W}$
1	.1278	.9950	.3628	1.0713	.3665	1.1142	.2807	1.0648	.1737	.9311
2	.0338	.4995	.1102	.5120	.1516	.5305	.1658	.5436	.1569	.5419
3	.0152	.3333	.0513	.3374	.0774	.3449	.0958	.3537	.1048	.3605
4	.0086	.2502	.0293	.2519	.0459	.2555	.0599	.2604	.0699	.2655
5	.0055	.2003	.0190	.2012	.0302	.2031	.0403	.2060	.0487	.2093
6	.0038	.1670	.0132	.1676	.0213	.1687	.0289	.1705	.0355	.1727
7	.0028	.1433	.0098	.1436	.0158	.1444	.0216	.1456	.0269	.1470
8	.0022	.1255	.0075	.1257	.0122	.1262	.0168	.1271	.0211	.1281
9	.0017	.1117	.0060	.1119	.0097	.1122	.0134	.1128	.0169	.1136
10	.0014	.1007	.0049	.1008	.0079	.1011	.0110	.1015	.0138	.1021

(b) η = .500

	m = 1		m = 2		m = 3		m = 4		m = 5	
n	$\bar{U}/\bar{W}$	$\bar{V}/\bar{W}$	$\bar{U}/\bar{W}$	$\bar{V}/\bar{W}$	$\bar{U}/\bar{W}$	$\bar{V}/\bar{W}$	$\bar{U}/\bar{W}$	$\bar{V}/\bar{W}$	$\bar{U}/\bar{W}$	$\bar{V}/\bar{W}$
1	.2368	.3466	.0097	.3720	-.0416	.1484	-.0399	.0796	-.0345	.0498
2	.1146	.4781	.1112	.4083	.0077	.2322	-.0178	.1397	-.0232	.0918
3	.0627	.3277	.1125	.3317	.0433	.2486	.0064	.1720	-.0085	.1212
4	.0384	.2480	.0901	.2612	.0577	.2303	.0249	.1806	.0056	.1373
5	.0256	.1922	.0690	.2105	.0587	.2023	.0356	.1745	.0169	.1424
6	.0182	.1665	.0531	.1748	.0539	.1754	.0400	.1617	.0245	.1401
7	.0136	.1430	.0416	.1491	.0474	.1525	.0405	.1469	.0289	.1335
8	.0105	.1253	.0332	.1298	.0411	.1339	.0387	.1327	.0309	.1249
9	.0084	.1115	.0271	.1149	.0355	.1189	.0360	.1198	.0311	.1158
10	.0069	.1005	.0224	.1032	.0307	.1067	.0329	.1086	.0303	.1070

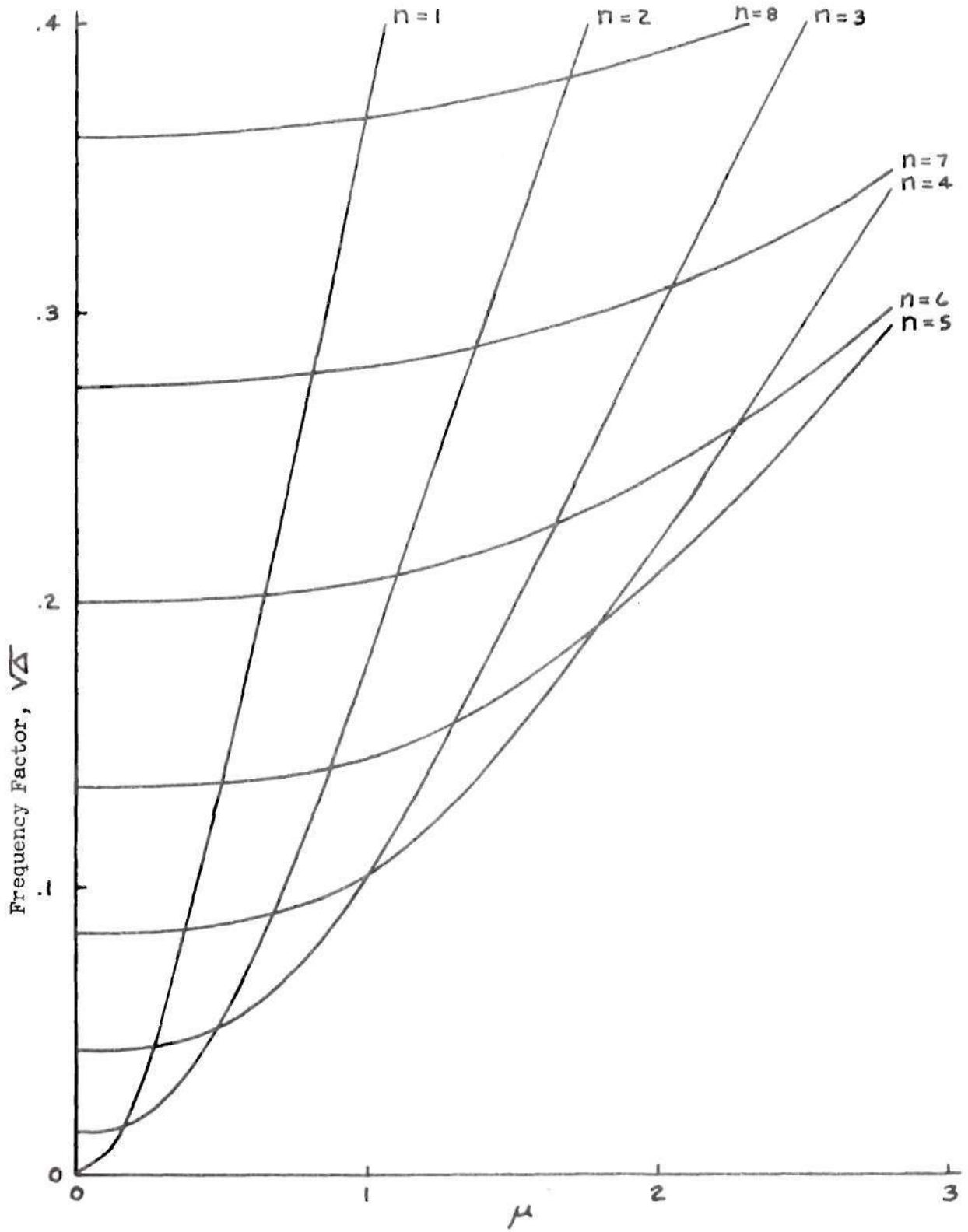

Figure 3. Frequency Factor For h/a = .020.

assumed to produce no middle surface strains. Separating the two parts and writing deformations in terms of the modal amplitudes $\bar{U}/\bar{W}$ and $\bar{V}/\bar{W}$, the following expression is obtained

$$\Omega = \ell \bar{W}^2 \left[\frac{E\pi}{4(1-\nu^2)}\right](\delta_s + \delta_B) \tag{27}$$

where δ_s and δ_B are energy factors for stretching and bending respectively,

$$\delta_s = 2\frac{h}{a}\Big\{ B_m^2\left[\eta^2\lambda_m^2 + \frac{(1-\nu)}{2}n^2(\gamma_m - M_m)\right]\left(\frac{\bar{U}}{\bar{W}}\right)^2 \tag{28}$$

$$-2\nu\eta A_m B_m M_m\left(\frac{\bar{U}}{\bar{W}}\right) + A_m^2\left[n^2 + \frac{(1-\nu)}{2}\eta^2\lambda_m(\gamma_m - M_m)\right]\left(\frac{\bar{V}}{\bar{W}}\right)^2$$

$$-2A_m^2 n\left(\frac{\bar{V}}{\bar{W}}\right) + \eta n A_m B_m\left[(1+\nu)M_m - (1-\nu)\gamma_m\right]\left(\frac{\bar{U}}{\bar{W}}\right)\left(\frac{\bar{V}}{\bar{W}}\right) + A_m^2\Big\}$$

$$\delta_B = 2\frac{h}{a}\beta A_m^2\Big\{\left[n^2 + 2(1-\nu)\eta^2\lambda_m(\gamma_m - M_m)\right]\left(\frac{\bar{V}}{\bar{W}}\right)^2 \tag{29}$$

$$+\left[-2n^3 + 2(2-\nu)n\eta^2\lambda_m M_m - 4(1-\nu)n\eta^2\lambda_m\gamma_m\right]\left(\frac{\bar{V}}{\bar{W}}\right)$$

$$+\left[n^4 + \eta^4\lambda_m^4 + 2(1-\nu)n^2\eta^2\lambda_m\gamma_m - 2n^2\eta^2\lambda_m M_m\right]\Big\}$$

Evaluation of δ_s and δ_B permits a comparison of the straining actions involved in any mode. Figure 4 (a, b) shows the energy factor distribution with circumferential mode number n, for h/a = .002 and two values of length factor, η. In Figure 4 (b) there is a sharp distinction between δ_s and δ_B except at n = 6, there the total energy factor is a minimum. Referring to Figure 2, the minimum value of $\sqrt{\Delta}$

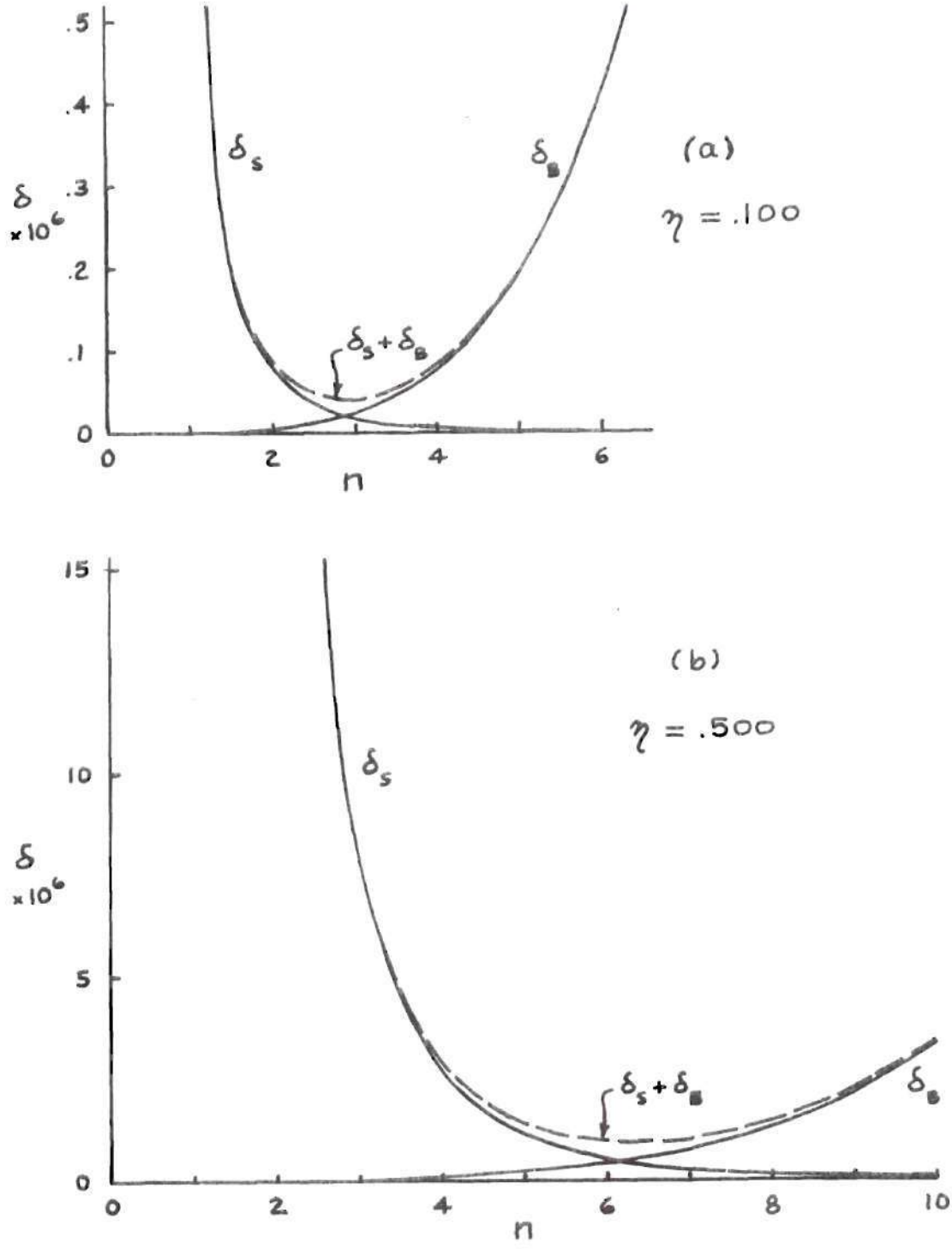

Figure 4. Energy Factor Versus Circumferential Mode Number For h/a = .002, m = 1.

at $\mu = .938$ is found to be on the n = 6 curve. The same result is found for Figure 4 (a), at $\mu = .188$ the minimum $\sqrt{\Delta}$ is at n = 3. These results are better defined in Appendix A, referring to Figure 8 and Figure 12, for $\eta = .1$ and $\eta = .5$ respectively. The results in Figure 4 apply only at integral values of n, the continuous lines in the graph being used for convenience of representation. An obvious result of Figure 5 is the sharp distinction between nodal patterns consisting primarily of bending deformations and those consisting primarily of stretching deformations. For shorter wavelength, that is for larger μ and η, stretching deformation predominates for progressively higher n. Figure 5 (a) demonstrates this for h/a = .002, n = 3, and for n = 6 in Figure 5 (b). It is noted that even for n = 6 the deformation is primarily stretching if the wavelength is sufficiently short.

Approximately 1000 computations of frequency factor, modal amplitudes and energy factors were made, for a range of thicknesses and lengths. An IBM 7094 digital computer was used for the computations. Appendix B presents sample calculations resulting from the computer study, showing values of all input parameters and for the three values of Δ.

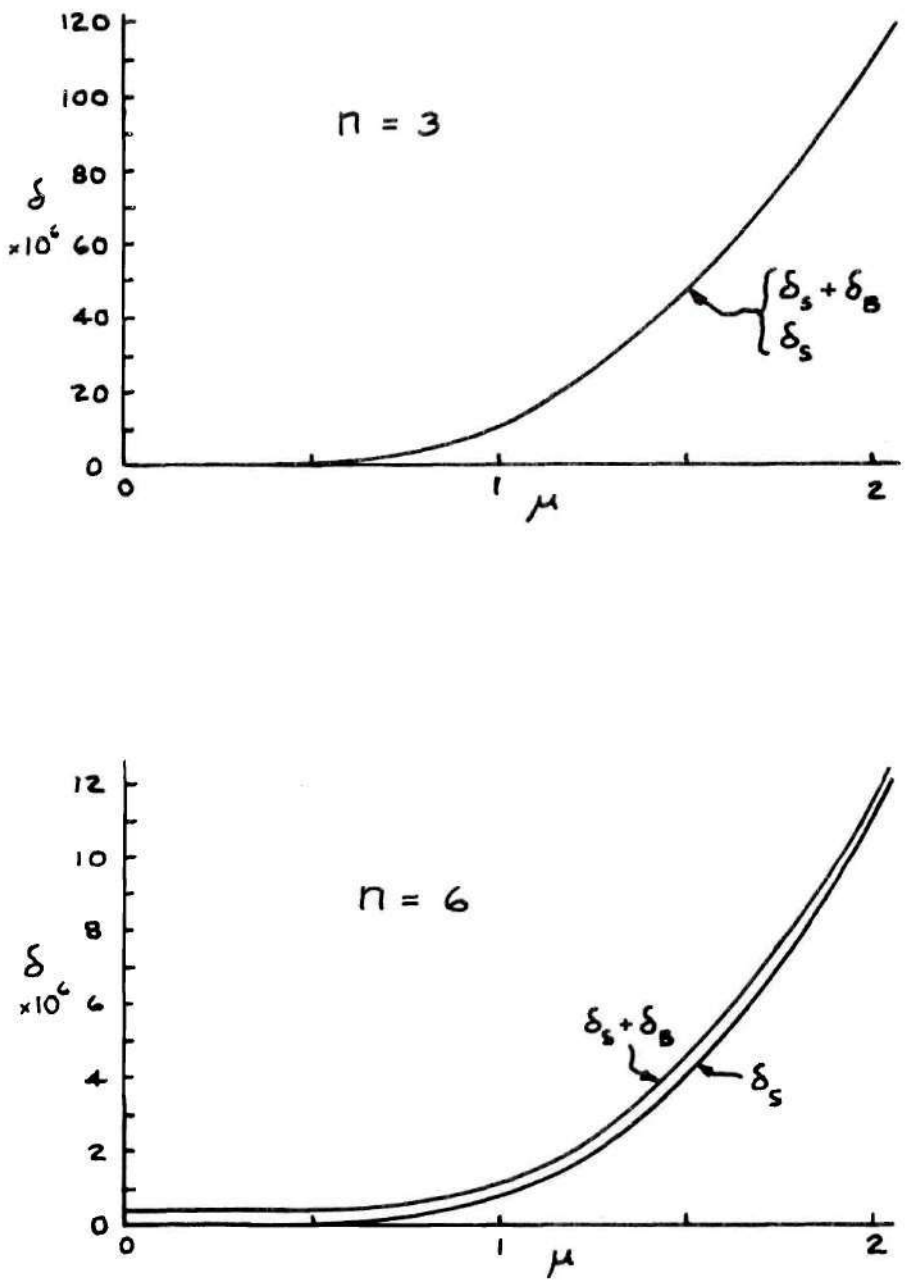

Figure 5. Energy Factor Versus Wavelength Factor, h/a = .002

CHAPTER III

EXPERIMENTAL INVESTIGATION

A limited experimental investigation was incorporated to determine the accuracy of the theoretical results. Since the higher modes in m and n converge to known results for a long simple supported shell, the purpose here is to verify the lower modes for relatively short shells.

An aluminum test article of h/a = .010 and a = 2.50 inches was constructed, using an Aluminum base plate. An aluminum bonding material was found satisfactory for attaining the built-in condition, with the shell resting in a thin slot in the base plate. Initial tests for this specimen were for η = .100. Later tests were run with the shell reduced in length to attain a value of η such that μ for m = 1 was equal to μ for m = 2 of the η = .100 shell. The frequencies were found to be identical for high axial mode numbers, consequently only the test data for η = .100 are presented in the summary graph. One test shell was constructed of stainless steel, for h/a = .010 and η = .500. In order to represent the clamped boundary a circular yoke and plug two inches thick was machined to fit one end of the shell.

The experimental setup used to survey the shell modes is shown schematically in Figure 6.

The modes detected in all the shells were in the low audio range and were considered to be sufficient to compare with theoretical results. The electromechanical driver was found to severely disturb mode patterns at frequencies beyond 1000 cycles per second and, as

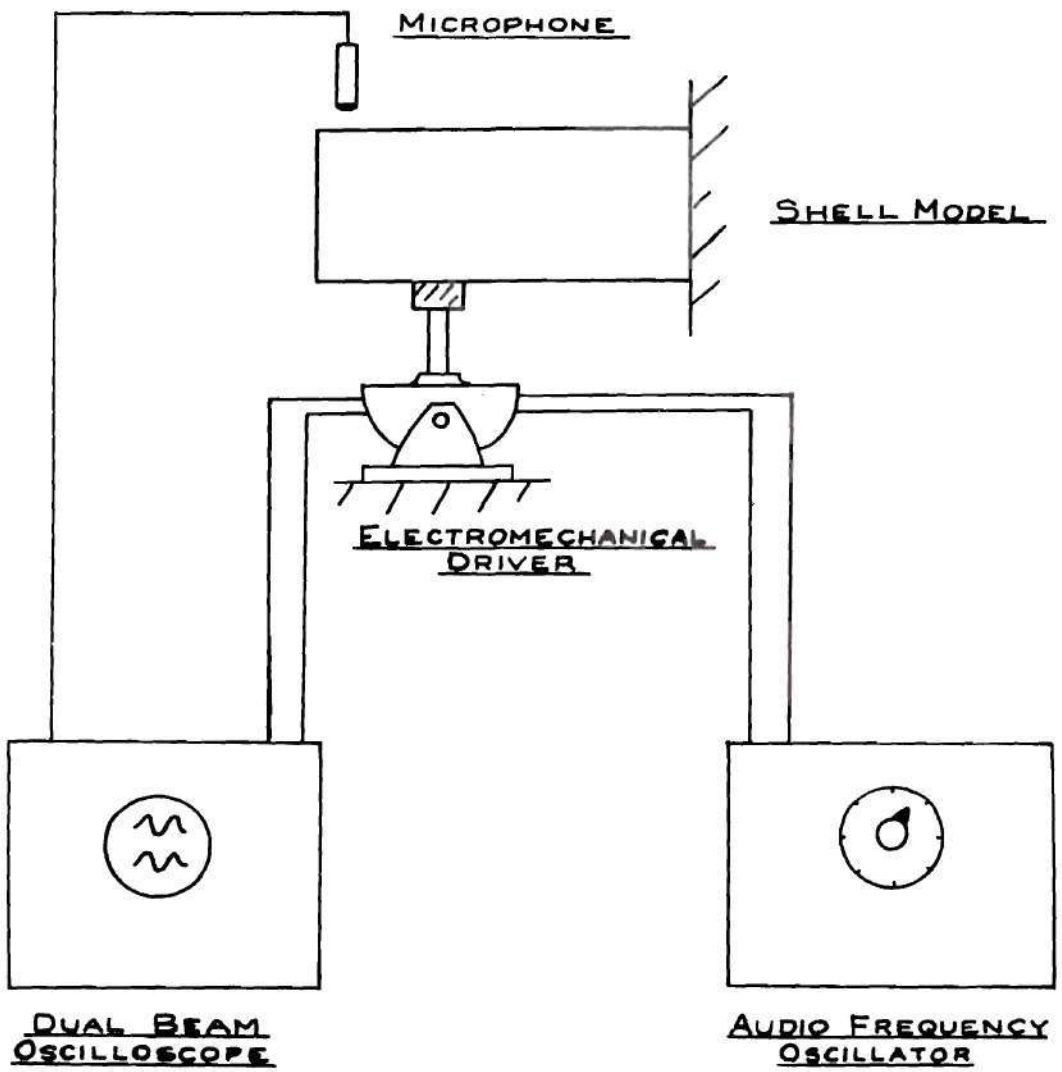

Figure 6. Schematic Diagram of Experimental Arrangement

experience now indicates, is not the most desirable method of excitation even for the lower frequencies. Testing with the steel shell was handicapped because of the higher frequencies involved.

The test results for all models are presented in Figure 7, where the solid lines are theoretical values for h/a = .010. In general the agreement between theory and test is fair, the theory generally giving higher values, as would be expected for any approximate energy approach. The highest percentage of error is in evidence for the low values of n. The author is convinced that this error is primarily due to the difficulty in representing the clamped boundary for the n = 2 and n = 3 modes. As stated in a previous section these modes are primarily stretch modes, and the clamping mechanism was not sufficient to entirely stop linear straining at the base. The effect of the clamp would then be to effectively increase the shell length. It is clear from Figure 7 that, due to the steep slope of the n = 2 and n = 3 curves, only a small decrease in η would shift the test points toward the origin, into better agreement with theory. A much better model would result from machining the shell integrally with the base. If such shells were constructed of steel, an electromagnetic device could be used to drive the vibrations and the modal pattern would then be undisturbed since no mechanical contact would be involved. Even under these conditions it would not be possible to verify the existence of the two higher eigenvalues predicted by theory, since they lie far outside the audio range, as indicated in Appendix B. Elaborate test methods would be required for detection, and, to the writer's knowledge this has not been done for any type of shell.

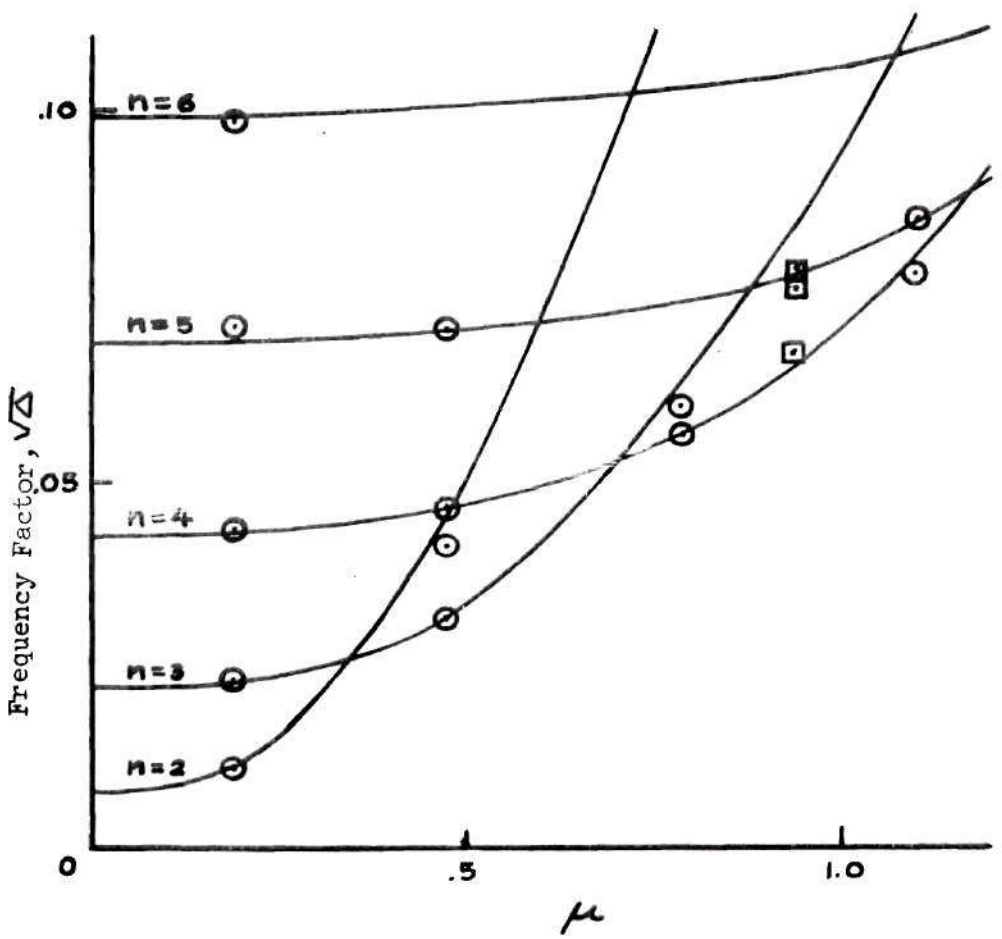

Figure 7. Comparison of Theoretical and Experimental Results For h/a = .010.

CHAPTER IV

CONCLUSIONS AND RECOMMENDATIONS

A theoretical method has been developed to predict the eigenvalues for a cantilevered circular cylindrical shell. The variation of eigenvalues with modal pattern is found to be complex, the "cross over" effect being more evident for thinner shells. This phenomenon is explained on the basis of energy distribution. It is shown that the method of determining eigenvalues is reduced to a practical engineering computation, not requiring the use of a high speed computer. Test results are considered sufficient to validate the analytical method.

It is recommended that more refined test procedures be developed to extend experimental results. For example, integral models would provide precise representation of the cantilever for the lower modes. Application of an electromagnetic driver would eliminate the coupling of the forcing mechanism with the shell. For larger models, acoustical forcing would be applicable, since a larger impingement area would absorb more sonic energy.

Due to the sensitivity of boundary clamping, a combined theoretical and experimental study is desirable to determine the relaxing effect of various structural ties, such as flanged ends, on the predicted cantilevered frequencies.

APPENDICES

APPENDIX A

ADDITIONAL FREQUENCY AND MODAL DATA

Figures 8 through 11 present graphs of frequency factor, $\sqrt{\Delta}$, versus radius to length ratio, η, with circumferential mode number, n, as parameter. The thickness ratio is h/a = .002, the axial mode number is specified and varies from m = 1 to m = 4 successively. Similar information is provided in Figures 12 through 15 for h/a = .020. This manner of presentation is desirable for use in practical computations, especially for short shells where primary response is in the first axial mode. Tables 4 and 5 present modal amplitudes for intermediate values of radius to length ratio, η = .167, .250, for h/a = .002 and h/a = .020 respectively.

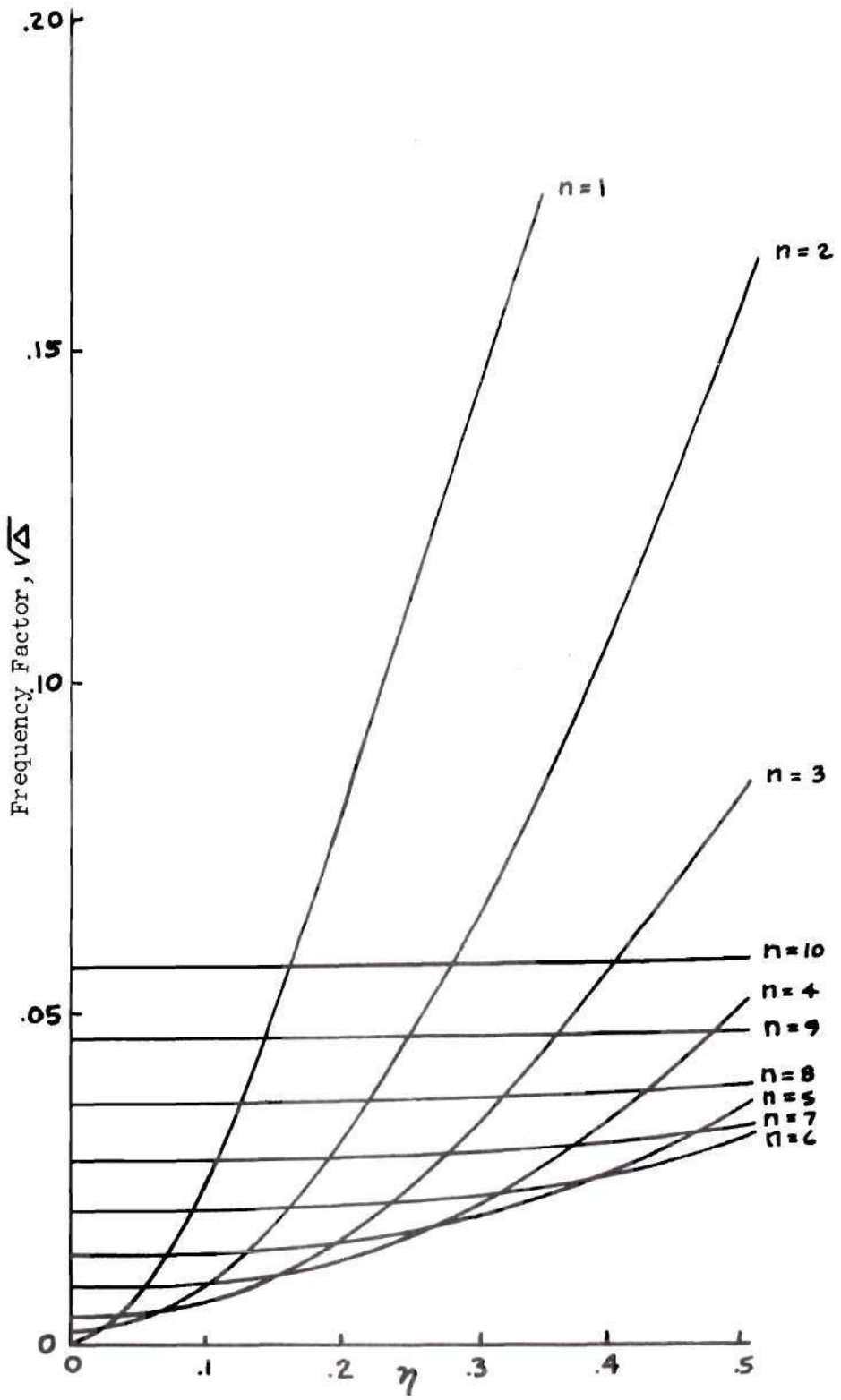

Figure 8. Frequency Factor Versus Radius To Length Ratio, h/a = .002, m = 1.

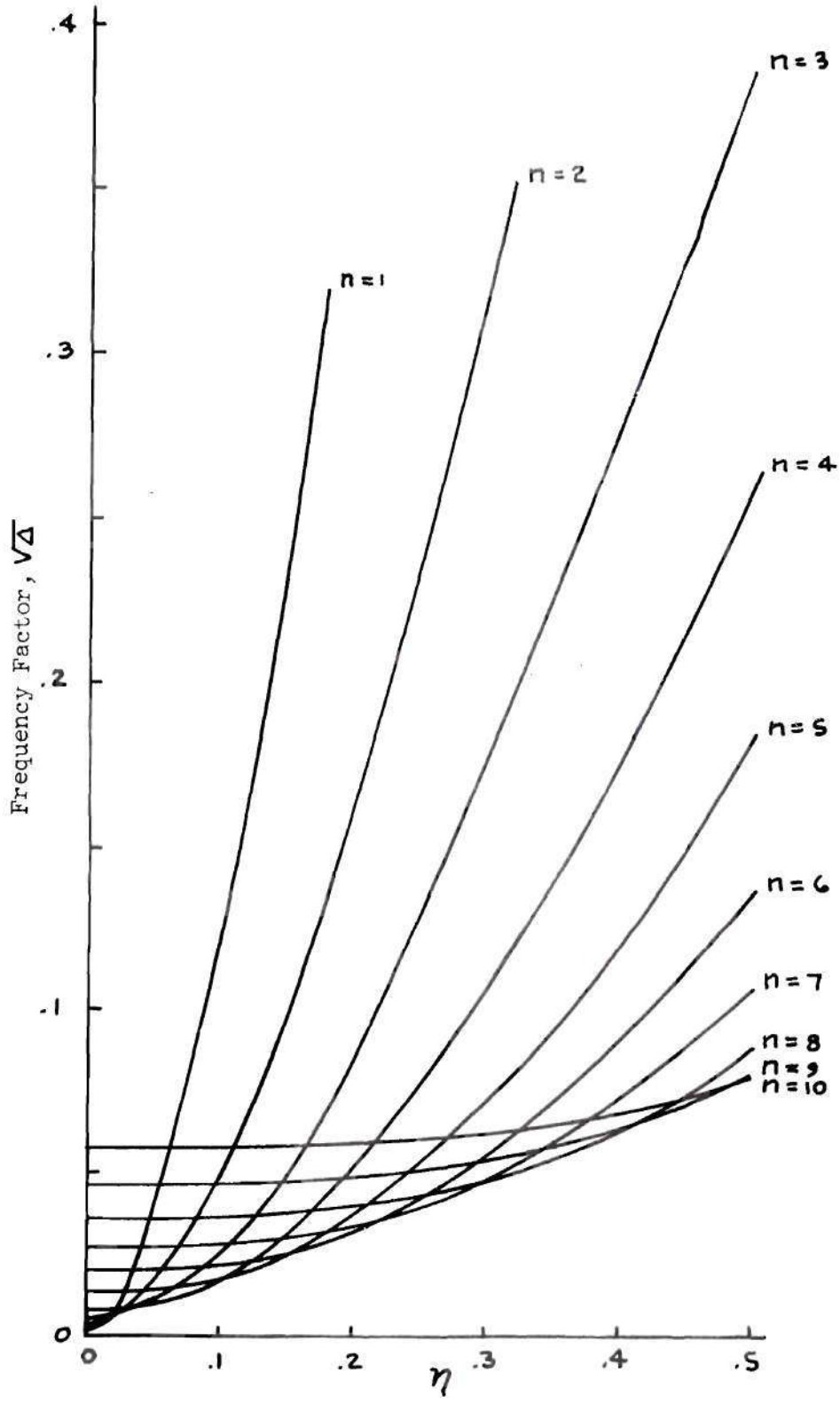

Figure 9. Frequency Factor Versus Radius To Length Ratio, h/a = .002, m = 2.

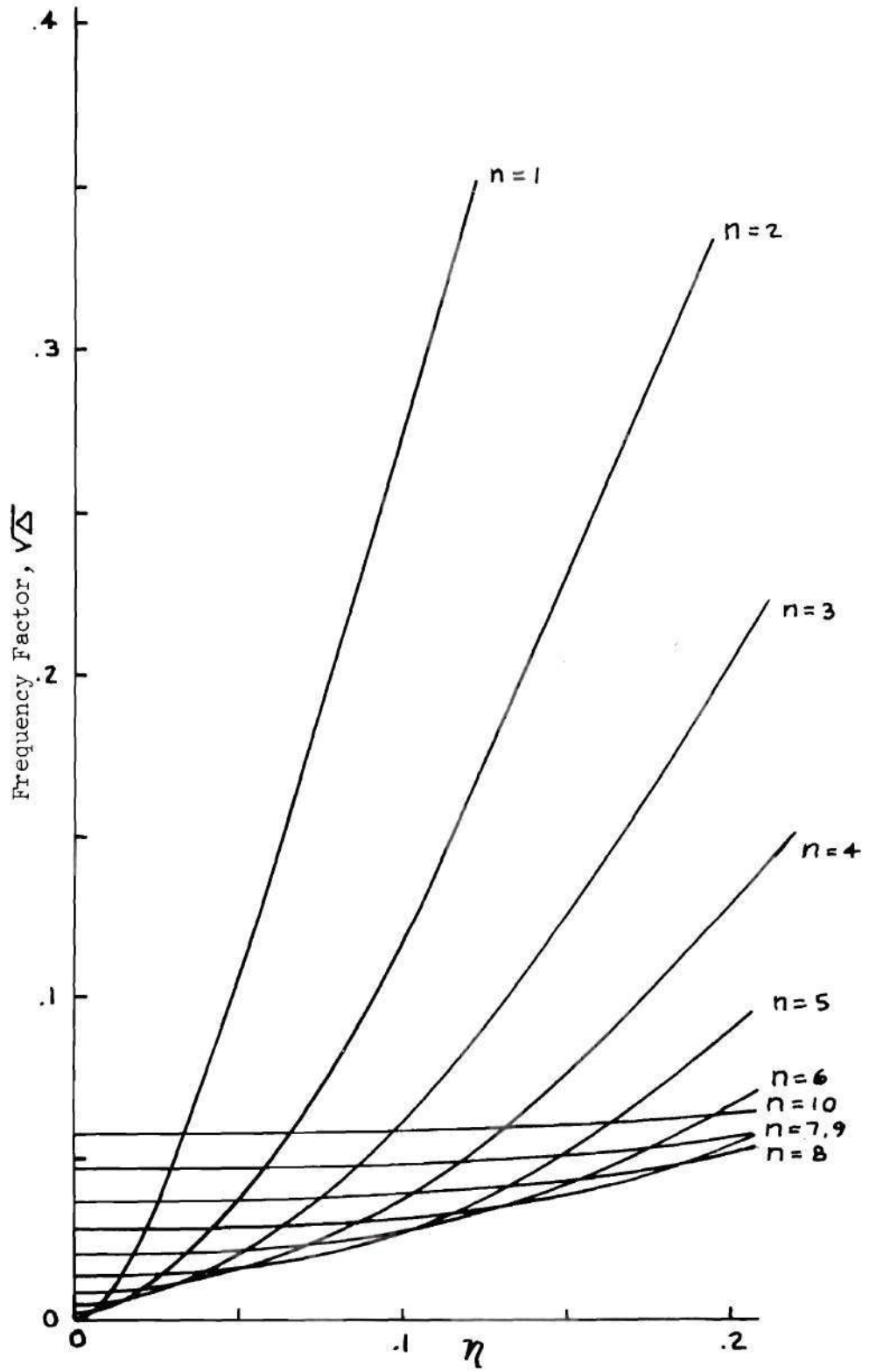

Figure 10. Frequency Factor Versus Radius To Length Ratio, h/a = .002, m = 3.

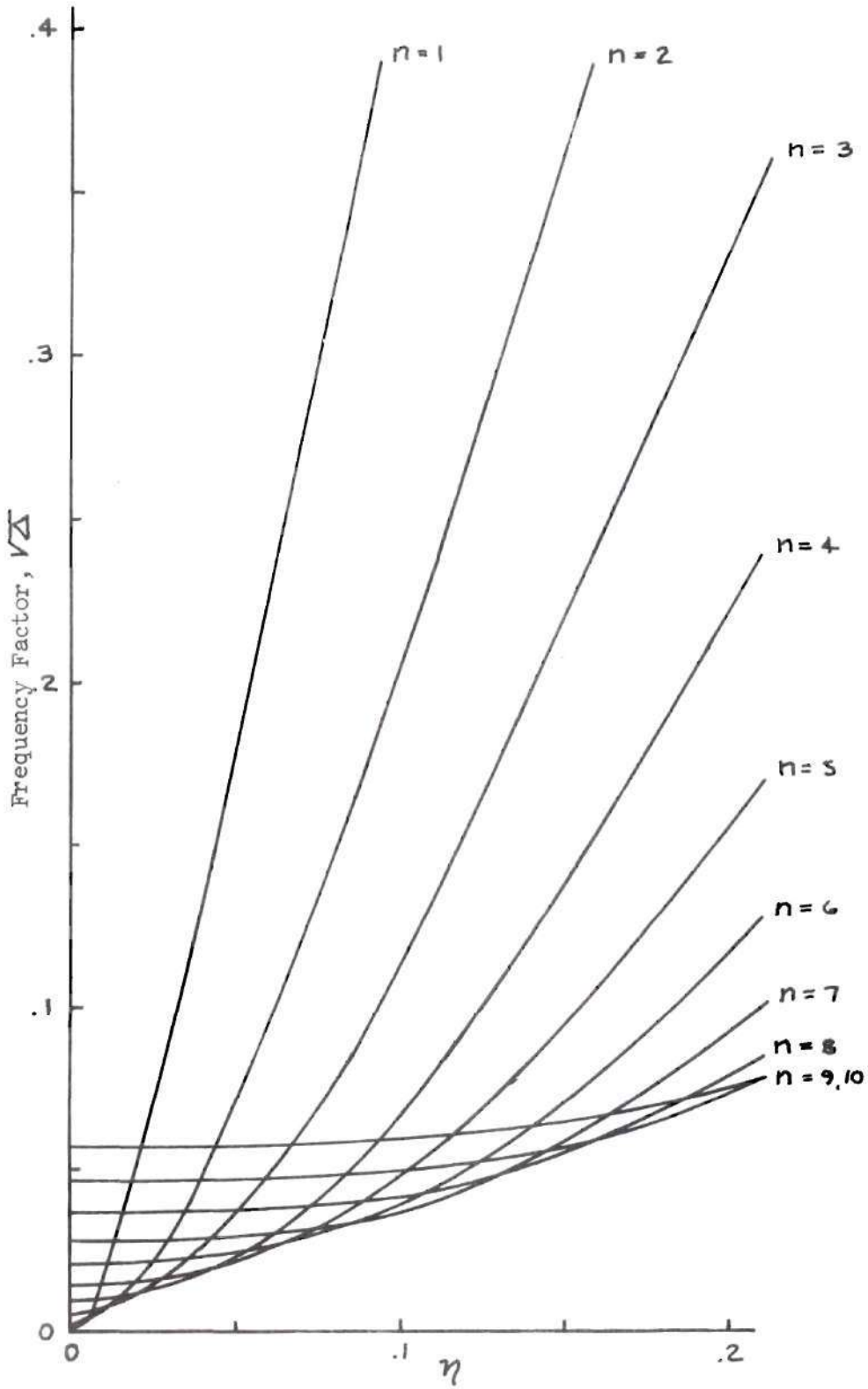

Figure 11. Frequency Factor Versus Radius To Length Ratio, h/a = .002, m = .4.

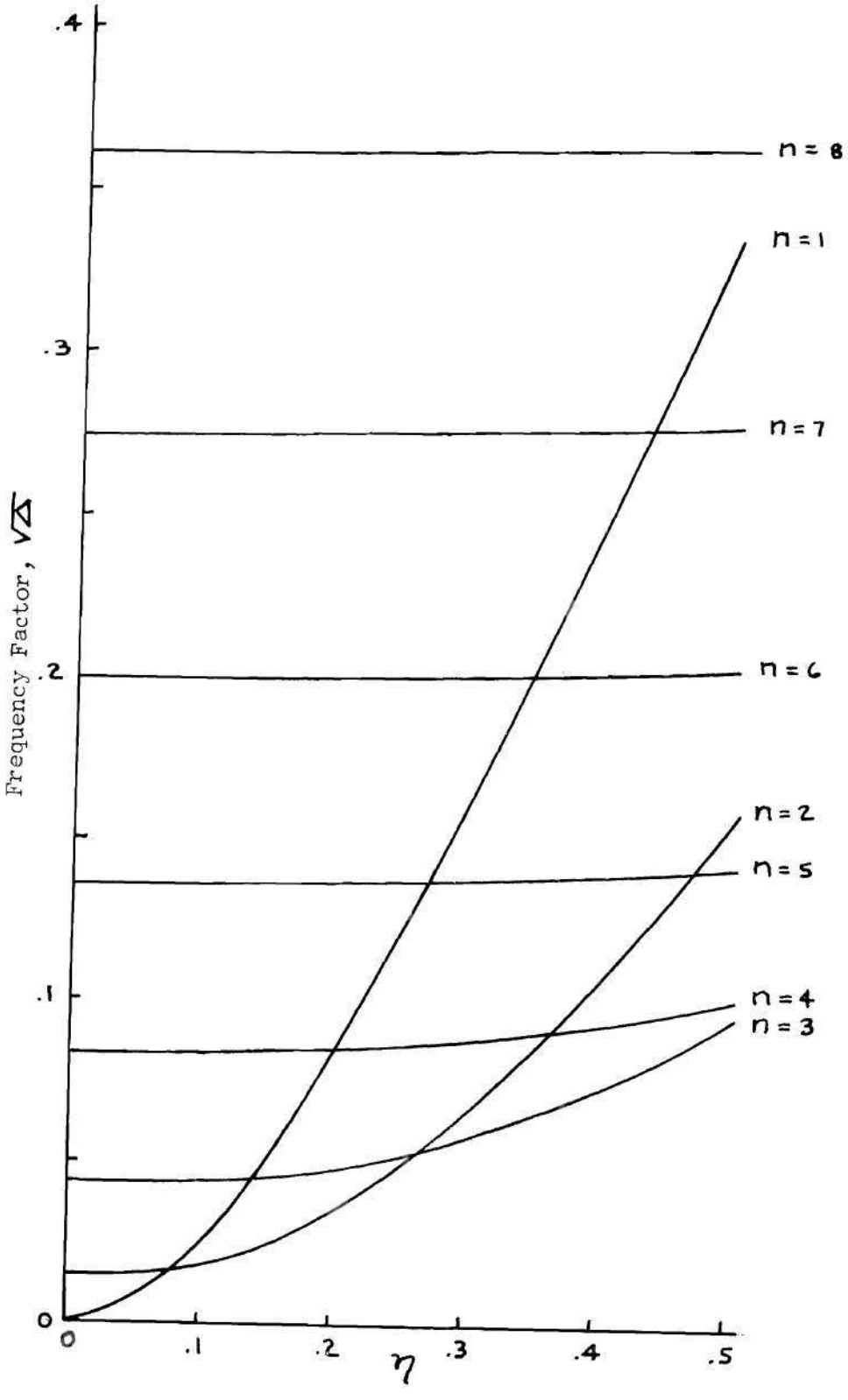

Figure 12. Frequency Factor Versus Radius To Length Ratio, h/a = .020, m = 1.

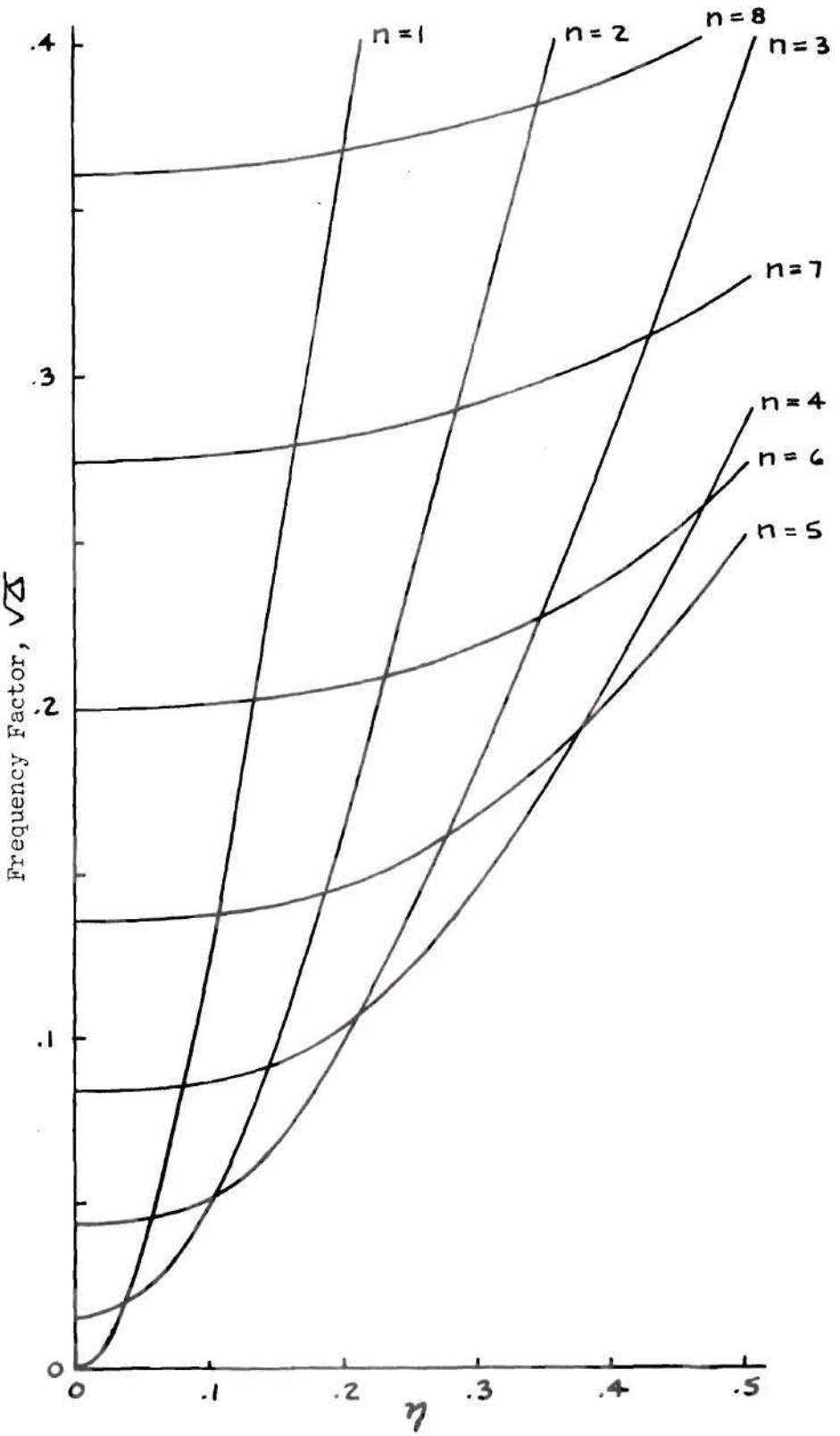

Figure 13. Frequency Factor Versus Radius To Length Ratio, h/a = .020, m = 2.

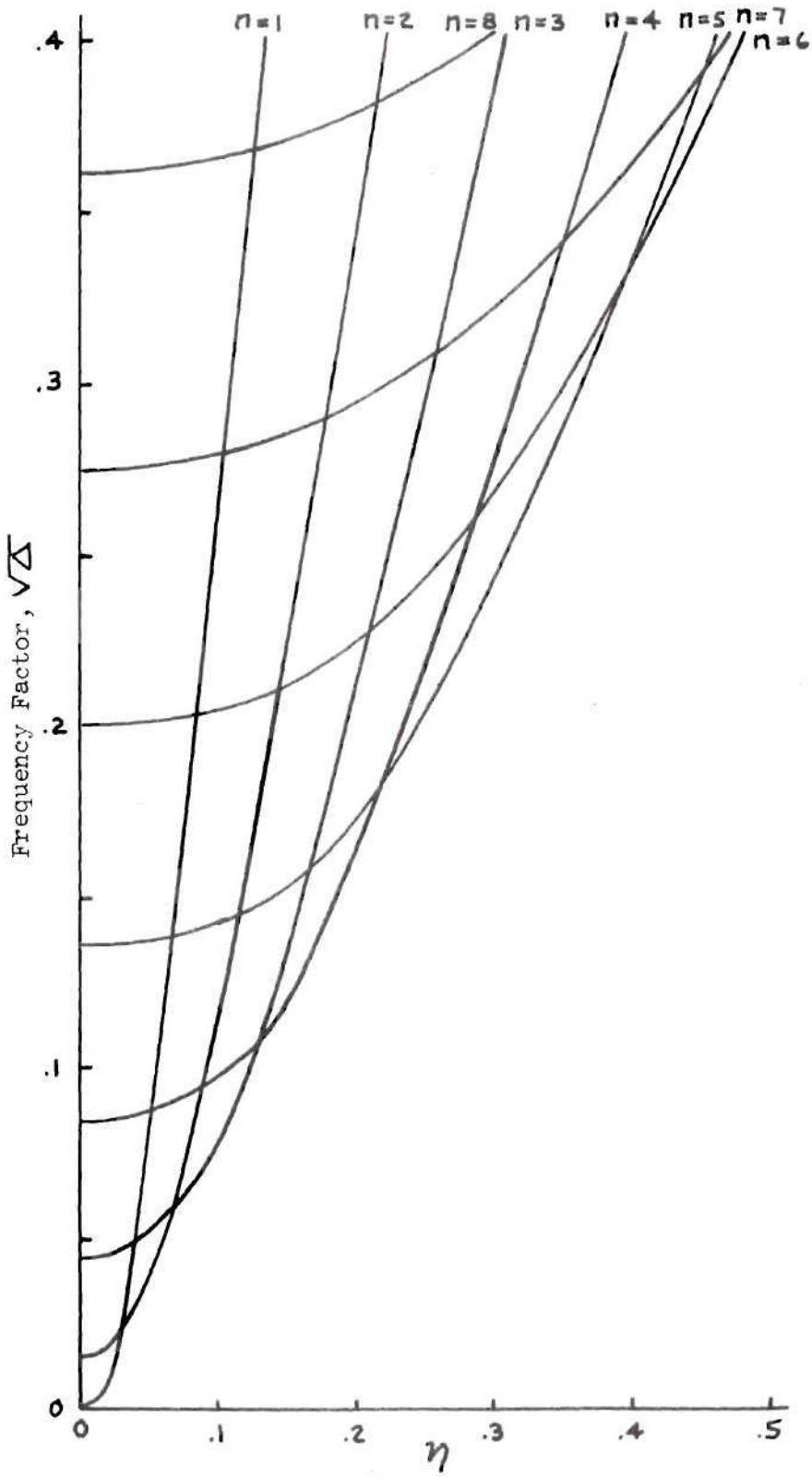

Figure 14. Frequency Factor Versus Radius To Length Ratio, h/a = .020, m = 3.

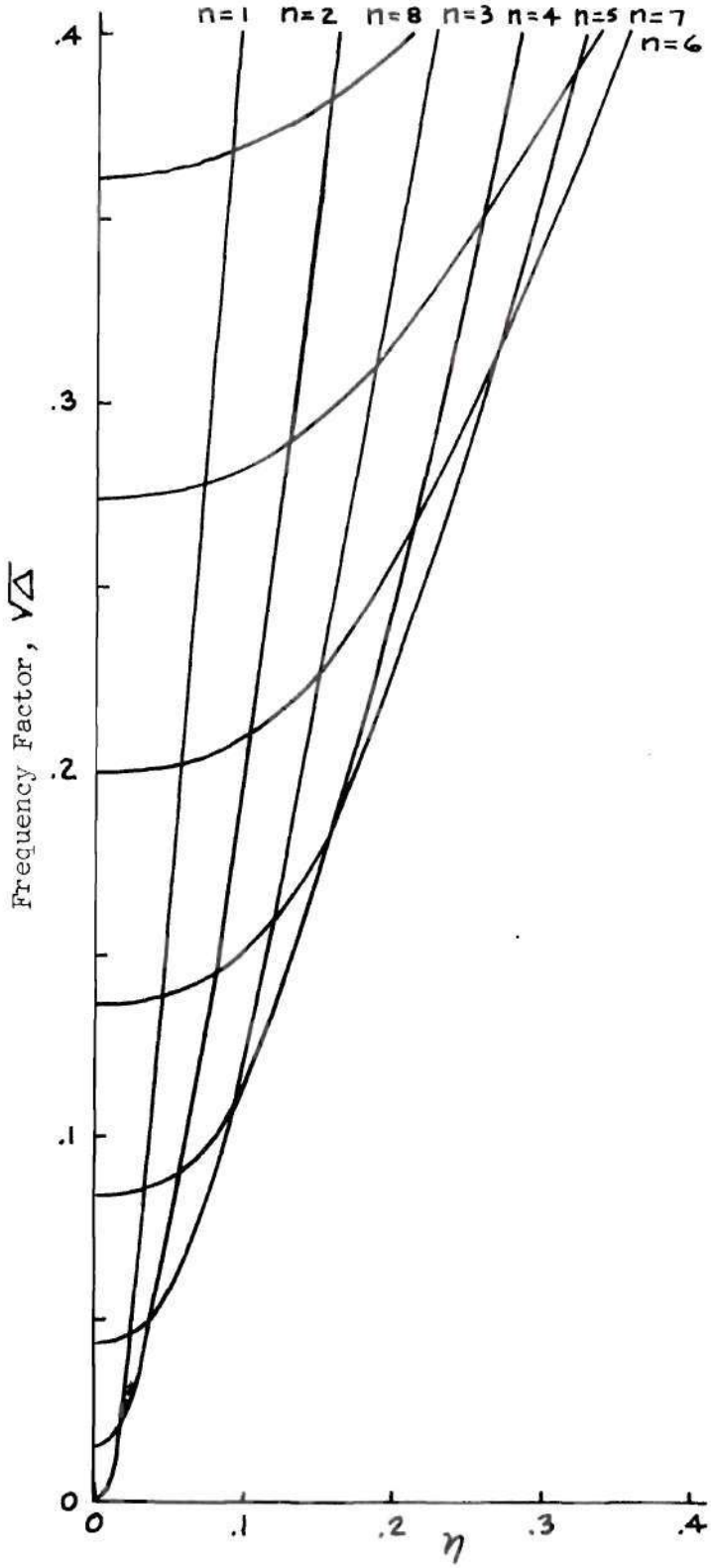

Figure 15. Frequency Factor Versus Radius To Length Ratio, h/a = .020, m = 4.

Table 4. Relative Modal Amplitudes, h/a = .002

η = .167

	m = 1		m = 2		m = 3		m = 4		m = 5	
n	$\bar{U}/\bar{W}$	$\bar{V}/\bar{W}$	$\bar{U}/\bar{W}$	$\bar{V}/\bar{W}$	$\bar{U}/\bar{W}$	$\bar{V}/\bar{W}$	$\bar{U}/\bar{W}$	$\bar{V}/\bar{W}$	$\bar{U}/\bar{W}$	$\bar{V}/\bar{W}$
1	.1898	.9854	.4169	1.0940	.2298	.9517	.0695	.6801	-.0075	.4588
2	.0545	.4982	.1600	.5248	.1689	.5351	.1322	.5052	.0849	.4445
3	.0249	.3328	.0801	.3427	.1051	.3547	.1075	.3583	.0938	.3480
4	.0142	.2498	.0471	.2543	.0678	.2617	.0784	.2682	.0789	.2698
5	.0091	.1999	.0307	.2023	.0464	.2068	.0572	.2119	.0623	.2156
6	.0064	.1666	.0216	.1680	.0334	.1709	.0428	.1745	.0488	.1779
7	.0047	.1428	.0160	.1437	.0251	.1456	.0330	.1482	.0387	.1509
8	.0036	.1250	.0123	.1256	.0195	.1269	.0260	.1288	.0312	.1309
9	.0028	.1111	.0098	.1115	.0156	.1125	.0210	.1139	.0255	.1155
10	.0023	.1000	.0079	.1003	.0127	.1010	.0172	.1021	.0212	.1033

η = .250

	m = 1		m = 2		m = 3		m = 4		m = 5	
n	$\bar{U}/\bar{W}$	$\bar{V}/\bar{W}$	$\bar{U}/\bar{W}$	$\bar{V}/\bar{W}$	$\bar{U}/\bar{W}$	$\bar{V}/\bar{W}$	$\bar{U}/\bar{W}$	$\bar{V}/\bar{W}$	$\bar{U}/\bar{W}$	$\bar{V}/\bar{W}$
1	.2350	.9649	.3339	.9905	.0519	.5873	-.0290	.3300	-.0458	.2053
2	.0766	.4957	.1860	.5288	.1277	.4814	.0586	.3930	.0156	.2898
3	.0363	.3321	.1058	.3490	.1090	.3521	.0825	.3273	.0511	.2846
4	.0209	.2495	.0656	.2582	.0812	.2664	.0769	.2642	.0613	.2490
5	.0135	.1998	.0440	.2047	.0599	.2114	.0642	.2148	.0590	.2113
6	.0094	.1665	.0313	.1695	.0451	.1744	.0521	.1786	.0522	.1794
7	.0070	.1428	.0234	.1447	.0348	.1482	.0422	.1520	.0449	.1541
8	.0053	.1250	.0181	.1263	.0275	.1288	.1345	.1318	.0382	.1343
9	.0042	.1111	.0144	.1120	.0223	.1139	.0285	.1163	.0325	.1186
10	.0034	.1000	.0117	.1007	.0183	.1021	.0239	.1040	.0278	.1060

Table 5. Relative Modal Amplitudes, h/a = .020

η = .167

	m = 1		m = 2		m = 3		m = 4		m = 5	
n	$\bar{U}/\bar{W}$	$\bar{V}/\bar{W}$	$\bar{U}/\bar{W}$	$\bar{V}/\bar{W}$	$\bar{U}/\bar{W}$	$\bar{V}/\bar{W}$	$\bar{U}/\bar{W}$	$\bar{V}/\bar{W}$	$\bar{U}/\bar{W}$	$\bar{V}/\bar{W}$
1	.1898	.9854	.4169	1.0940	.2298	.9517	.0695	.6801	-.0075	.4588
2	.0545	.4982	.1600	.5248	.1689	.5351	.1322	.5052	.0849	.4445
3	.0250	.3328	.0801	.3427	.1051	.3547	.1075	.3583	.0938	.3480
4	.0142	.2498	.0471	.2543	.0678	.2617	.0784	.2682	.0789	.2698
5	.0091	.1999	.0307	.2023	.0464	.2068	.0572	.2119	.0673	.2156
6	.0064	.1666	.0216	.1680	.0334	.1709	.0248	.1745	.0488	.1780
7	.0047	.1429	.0160	.1437	.0251	.1456	.0330	.1482	.0387	.1510
8	.0036	.1250	.0123	.1256	.0195	.1269	.0260	.1288	.0312	.1309
9	.0028	.1110	.0098	.1115	.0156	.1125	.0210	.1139	.0255	.1155
10	.0023	.1000	.0079	.1003	.0127	.1010	.0172	.1021	.0212	.1033

η = .250

	m = 1		m = 2		m = 3		m = 4		m = 5	
n	$\bar{U}/\bar{W}$	$\bar{V}/\bar{W}$	$\bar{U}/\bar{W}$	$\bar{V}/\bar{W}$	$\bar{U}/\bar{W}$	$\bar{V}/\bar{W}$	$\bar{U}/\bar{W}$	$\bar{V}/\bar{W}$	$\bar{U}/\bar{W}$	$\bar{V}/\bar{W}$
1	.2350	.9650	.3339	.9905	.0519	.5873	-.0290	.3300	-.0458	.2053
2	.0766	.4957	.1860	.5287	.1277	.4814	.0586	.3830	.0156	.2898
3	.0363	.3321	.1058	.3490	.1090	.3521	.0825	.3273	.0511	.2846
4	.0209	.2495	.0656	.2582	.0812	.2664	.0769	.2642	.0613	.2490
5	.0135	.1998	.0440	.2047	.0599	.2114	.0642	.2148	.0590	.2113
6	.0094	.1665	.0313	.1695	.0451	.1744	.0521	.1786	.0522	.1794
7	.0070	.1428	.0234	.1447	.0348	.1481	.0422	.1519	.0449	.1541
8	.0053	.1250	.0181	.1263	.0275	.1288	.0345	.1318	.0382	.1343
9	.0042	.1111	.0144	.1120	.0222	.1140	.1285	.1163	.0325	.1186
10	.0034	.1000	.0117	.1007	.0183	.1021	.0239	.1040	.0278	.1060

APPENDIX B

SAMPLE CALCULATIONS FROM DIGITAL COMPUTER PROGRAM

Tables 6 through 13 present complete input and output data, for several representative cases, from a digital computer program (Fortran language, IBM 7094 scientific computer). The "Geometric element" comment identifies the parameters h/a and η respectively, thus the array

h/a \ η	.100	.167	.250	.500
.002	1 - 1	1 - 2	1 - 3	1 - 4
.010	2 - 1	2 - 2	2 - 3	2 - 4
.020	3 - 1	3 - 2	3 - 3	3 - 4
.040	4 - 1	4 - 2	4 - 3	4 - 4

identifies for each geometric element the value of h/a and η. The axial and circumferential mode numbers are identified, the examples given are all for m = 1, n = 2,4. Input data is listed, along with the computed coefficients occurring in the frequency equation. Study of the numerical values of these coefficients reveals that S_{13} and S_{31} are small compared to the other s and b coefficients, however, it cannot be recommended that they be neglected in general since L_1, L_2, and L_3 are dependent on small differences in most cases. When using a desk calculator it is recommended that ten significant figures be retained in computing L_1, L_2, and L_3.

The three roots of the frequency equation are listed, along with the square root of the smallest of these, $\sqrt{\Delta}$. Finally the modal amplitudes $\overline{U}/\overline{W}$ (UBAR) and $\overline{V}/\overline{W}$ (VBAR) are listed, and the energy factors, δ_S (DS) and δ_B (DB). For the cases shown the large difference between the experimentally verified frequency factor and the other two roots is apparent. The smallest difference between the frequency factors occurs for the short shell at low values of n. The smallest difference being a factor of ten on the frequency. However, for a reasonable size of shell model the lowest root already lies close to the audio limit (approximately 16 KC).

Table 6. Computed Data for Element One-One, m=1, n=2

GEOMETRIC ELEMENT ONE-ONE

M=1

N =	2	BETA =	0.33329999E-06	NU =	0.30000000E-00
		LAMBDA =	0.18750999E 01	ETA =	0.09999999E-00
		ZETA =	0.29363800E 01	MM =	0.45767000E-00
		AM =	0.50000000E 00	BM =	0.68110999E 00

S11 =	0.14265978E 01	B22 =	0.40650695E 01	L1 =	0.64428719E 01
S12 =	-0.58921576E 00	B23 =	-0.81249900E 01	L2 =	0.71562068E 01
S13 =	-0.55392118E-01	B33 =	0.16240918E 02	L3 =	0.44755175E-03
S21 =	-0.27385741E-01				
S22 =	0.40162673E 01				
S31 =	-0.25745309E-02				

ROOTS ARE

0.50162985E 01
0.62763691E-04
0.14265104E 01

SORT. MIN. POS. DELTA

0.79223539E-02

UBAR = 0.33752856E-01 VBAR = 0.49938960E-00

DS = 0.75574908E-07 DB = 0.30460878E-08

Table 7. Computed Data for Element One-One, m=1, n=4

GEOMETRIC ELEMENT ONE-ONE

M=1

N = 2

BETA	=	0.33329999E-06	NU	=	0.30000000E-00
LAMBDA	=	0.18750999E 01	ETA	=	0.09999999E-00
ZETA	=	0.29363800E 01	MM	=	0.45767000E-00
AM	=	0.50000000E 00	BM	=	0.68110999E 00

S11	=	0.56265979E 01	B22	=	0.16065069E 02	L1	= 0.22642956E 02
S12	=	-0.11784315E 01	B23	=	-0.64249980E 02	L2	= 0.95696989E 02
S13	=	-0.55392118E-01	B33	=	0.25695996E 03	L3	= 0.72058346E-02
S21	=	-0.54771481E-01					
S22	=	0.16016267E 02					
S31	=	-0.25745309E-02					

ROOTS ARE

0.17020538E 02
0.76174736E-04
0.56223404E 01

SORT. MIN. POS. DELTA

0.87278139E-02

UBAR = 0.85614734E-02 VBAR = 0.24992753E-00

DS = 0.47606828E-08 DB = 0.75271294E-07

Table 8. Computed Data for Element One-Four, m=1, n=2

GEOMETRIC ELEMENT ONE-FOUR

M=1

N =	2	BETA =	0.33329999E-06	NU =	0.30000000E-00
		LAMBDA =	0.18750999E 01	ETA =	0.50000000E 00
		ZETA =	0.29363800E 01	MM =	0.45767000E-00
		AM =	0.50000000E 00	BM =	0.68110999E 00

S11 =	0.20649478E 01	B22 =	0.56267401E 01	L1 =	0.74716422E 01
S12 =	-0.58921576E 00	B23 =	0.11124753E 02	L2 =	0.11164279E 02
S13 =	-0.55392118E-01	B33 =	0.22764695E 02	L3 =	0.26901304E-00
S21 =	-0.68464353E 00				
S22 =	0.44066849E 01				
S31 =	-0.64363275E-01				

ROOTS ARE

0.54215551E 01
0.24496526E-01
0.20255905E 01

SORT. MIN. POS. DELTA

0.15651365E-00

UBAR = 0.11455801E-00 VBAR = 0.47795666E-00

DS = 0.30961119E-04 DB = 0.44712565E-08

Table 9. Computed Data for Element One-Four, m=1, n=4

GEOMETRIC ELEMENT ONE-FOUR

M=1

N = 2

BETA	=	0.33329999E-06	NU	=	0.30000000E-00
LAMBDA	=	0.18750999E 01	ETA	=	0.50000000E 00
ZETA	=	0.29363800E 01	MM	=	0.45767000E-00
AM	=	0.50000000E 00	BM	=	0.68110999E 00

S11	=	0.62649478E 01	B22	=	0.17626739E 02	L1	= 0.23671731E 02
S12	=	-0.11784315E 01	B23	=	0.70249507E 02	L2	= 0.10784345E 03
S13	=	-0.55392118E-01	B33	=	0.28074086E 03	L3	= 0.27729826E-00
S21	=	-0.13692870E 01					
S22	=	0.16406684E 02					
S31	=	-0.64363275E-01					

ROOTS ARE

0.17515662E 02
0.25739670E-02
0.61534946E 01

SORT. MIN. POS. DELTA

0.50734278E-01

UBAR = 0.38269595E-01 VBAR = 0.24773393E-00

DS = 0.26666603E-05 DB = 0.82326405E-07

Table 10. Computed Data for Element Three-One, m=1, n=2

GEOMETRIC ELEMENT THREE-ONE

M=1

N = 2

BETA	=	0.33329999E-04	NU	=	0.30000000E-00
LAMBDA	=	0.18750999E 01	ETA	=	0.09999999E-00
ZETA	=	0.29363800E 01	MM	=	0.45767000E-00
AM	=	0.50000000E 00	BM	=	0.68110999E 00

S11	=	0.14265978E 01	B22	=	0.40650695E 01	L1	= 0.64435420E 01
S12	=	-0.58921576E 00	B23	=	-0.81249900E 01	L2	= 0.71583767E 01
S13	=	-0.55392118E-01	B33	=	-0.16240918E 02	L3	= 0.21700286E-02
S21	=	-0.27385741E-01					
S22	=	0.40162673E 01					
S31	=	-0.25745309E-02					

ROOTS ARE

0.50167261E 01
0.30350685E-03
0.14265122E 01

SORT. MIN. POS. DELTA

o.17421447E-01

UBAR = 0.33763133E-01 VBAR = 0.49947008E-00

DS = 0.75418454E-06 DB = 0.30457608E-05

Table 11. Computed Data for Element Three-One, m=1, n=4

GEOMETRIC ELEMENT THREE-ONE

M=1

N = 4

BETA	=	0.33329999E-04	NU	=	0.30000000E-00
LAMBDA	=	0.18750999E 01	ETA	=	0.09999999E-00
ZETA	=	0.29363800E 01	MM	=	0.45767000E-00
AM	=	0.50000000E 00	BM	=	0.68110999E 00

S11	=	0.56265979E 01	B22	=	0.16065069E 02	L1	= 0.22651964E 02
S12	=	-0.11784315E 01	B23	=	-0.64249980E 02	L2	= 0.95867047E 02
S13	=	-0.55392118E-01	B33	=	0.25695996E 03	L3	= 0.67828704E 00
S21	=	-0.54771481E-01					
S22	=	0.16016267E 02					
S31	=	-0.25745309E-02					

ROOTS ARE

0.17022531E 02
0.70880651E-02
0.56223442E 01

SORT. MIN. POS. DELTA

0.84190647E-01

UBAR = 0.85789125E-02 VBAR = 0.25016153E-00

DS = 0.54163011E-07 DB = 0.75261901E-04

Table 12. Computed Data for Element Three-Four, m=1, n=2

GEOMETRIC ELEMENT THREE-FOUR

M=1

N = 2 BETA = 0.33329999E-04 NU = 0.30000000E-00
LAMBDA = 0.18750999E 01 ETA = 0.50000000E 00
ZETA = 0.29363800E 01 MM = 0.45767000E-00
AM = 0.50000000E 00 BM = 0.68110999E 00

S11 = 0.20649478E 01 B22 = 0.56267401E 01 L1 = 0.74725790E 01
S12 = -0.58921576E 00 B23 = -0.11124753E 02 L2 = 0.11168241E 02
S13 = -0.55392118E-01 B33 = 0.22764695E 02 L3 = 0.27286813E-00
S21 = -0.68464353E 00
S22 = 0.44066849E 01
S31 = -0.64363275E-01

ROOTS ARE
0.54220959E 01
0.24844497E-01
0.20256384E 01

SORT. MIN. POS. DELTA

0.15762137E-00

UBAR = 0.30960412E-03 VBAR = 0.47806678E-00

DS = 0.30960412E-03 DB = 0.44706373E-05

Table 13. Computed Data for Element Three-Four, m=1, n=4

GEOMETRIC ELEMENT THREE-FOUR

M=1

N = 4 BETA = 0.33329999E-04 NU = 0.30000000E-00
LAMBDA = 0.18750999E 01 ETA = 0.50000000E 00
ZETA = 0.29363800E 01 MM = 0.45767000E-00
AM = 0.50000000E 00 BM = 0.68110999E 00

S11 = 0.62649478E 01 B22 = 0.17626739E 02 L1 = 0.23681577E 02
S12 = -0.11784315E 01 B23 = -0.70249507E 02 L2 = 0.10803916E 03
S13 = -0.55392118E-01 B33 = 0.28074086E 03 L3 = 0.11016332E 01
S21 == -0.13692870E 01
S22 = 0.16406684E 02
S31 = -0.64363275E-01

ROOTS ARE
0.17517759E 02
0.10220349E-01
0.61535963E 01

SORT. MIN. POS. DELTA

0.10109574E-00

UBAR = 0.38349856E-01 VBAR = 0.24799084E-00

DS = 0.26620561E-04 DB = 0.82315123E-04

BIBLIOGRAPHY

1. S. Timoshenko and S. Woinowsky-Krieger, Theory of Plates and Shells, McGraw-Hill Book Co., Inc., New York, N. Y., 1959.

2. S. Timoshenko, Vibration Problems in Engineering, D. Van Nostrand Co., Inc., New York, N. Y.

3. R. N. Arnold and G. B. Warburton, "Flexural Vibrations of the Walls of Thin Cylindrical Shells Having Freely Supported Ends," Proceedings of the Royal Society of London, England, Series A, Vol. 197 (1949), pp. 238-256.

4. R. N. Arnold, G. B. Warburton, "The Flexural Vibrations of Thin Cylinders," Proceedings of the Institution of Mechanical Engineers, Vol. 167, (1953), pp. 62.74.

5. Bernard Budiansky, Edwin T. Kruszewski, "Transverse Vibrations of Hollow Thin-Walled Cylindrical Beams," NACA TR 1129 (1953), Langley Aeronautical Laboratory, Langley Field, Virginia.

6. Yi-Yuan Yu, "Free Vibrations of Thin Cylindrical Shells Having Finite Lengths with Freely Supported and Clamped Edges," Journal of Applied Mechanics, Trans. ASME, (December, 1955), pp. 547-551.

7. Dana Young and Robert P. Felgar, Jr., "Tables of Characteristic Functions Representing Normal Modes of Vibration of A Beam," The University of Texas, Publication No. 4913, Engineering Research Series No. 44.

8. W. Flugge, Stresses in Shells, Springer-Verlag, Berlin (1960).

9. H. H. Bleich and F. Dimaggio, "A Strain Energy Expression for Thin Cylindrical Shells," Journal of Applied Mechanics, Vol. 20, (September, 1953), pp. 448-449.